Modeling the Multinuclear Redox-Active Manganese Enzymes. Synthesis, Structure, and Properties of a Bis(dinuclear Mn(III)−μ-oxo−bis(μ-acetato)) Complex

Yilma Gultneh,*,† Bijan Ahvazi,† A. Raza Khan,† Ray J. Butcher,† and J. P. Tuchagues‡

Department of Chemistry, Howard University, Washington, D.C. 20059, and Centre National de la Recherche Scientifique, UPR 8241, liee par conventions a l'Universite Paul Sabatier et a l'Institut National Polytechnique, 205 route de Narbonne, 31077 Toulouse Cedex, France

Received January 27, 1995[⊗]

The tetranuclear Mn(III) complex $[Mn^{III}_4L_2(\mu\text{-}O)_2(\mu\text{-}OAc)_4][(ClO_4)_4\cdot 3CH_3NO_2$ (L = α,α′-bis(bis(2-pyridylmethyl)-amino)-*m*-xylene), **2**, has been synthesized, and its structural, spectroscopic, and magnetic properties have been investigated. The kinetics of the reaction of its precursor Mn(II) complex (formulated as $[Mn_2L(OAc)_2(CH_3OH)](ClO_4)_2$, **1**, with O_2 that leads to the formation of **2** have been studied. Complex **2** crystallizes on the orthorhombic crystal system, space group *Pnma*, with the cell dimensions $a = 24.755(5)$ Å, $b = 28.854(4)$ Å, $c = 12.495(2)$ Å, and $Z = 4$. The structure shows four Mn(III) ions in a dimer of two dinuclear centers. Each dinuclear center has two Mn(III) ions triply bridged by two acetate groups and one oxo group with three nitrogen donors coordinated, forming a distorted octahedral coordination. The two dinuclear units are related to each other by a mirror plane. Within a dinuclear unit, the two Mn(III) ions show coordination differences in bond angles and bond distances arising from differences in the Jahn−Teller and lattice distortions of the octahedral coordination. Temperature-dependent magnetic susceptibility studies show very weak magnetic coupling ($J = -0.4$ cm^{-1}) between Mn(III) ions. The stoichiometry of the O_2/complex **1** reaction to form complex **2**, the EPR, molar conductance, and magnetic susceptibility studies, and the structural data for complex **2** all support the formulation of complex **2** as having four Mn(III) ions. IR spectral studies of samples of complex **2** prepared by the reaction of complex **1** with isotopically pure $^{16}O_2$ and $^{18}O_2$ show that the bridging oxo group is derived from dioxygen. Kinetic studies show that the reaction of the precursor Mn(II) complex **1** with O_2 is first order in the concentrations of both the dinuclear Mn(II) complex and O_2. The reactivity of the Mn(II) complex **1** with O_2 is in contrast to the lack of any reaction with O_2 under ordinary conditions of the Mn(II) complexes of dinucleating ligands with two bis(2-pyridylmethyl)amine donor groups connected by straight-chain hydrocarbons (C(3) to C(5)). The rigidity of the *m*-xylene group connecting the two donor sets in the ligand L of complex **1** may be responsible for the contribution of the critical entropic factor in favor of the reaction, which may account for this difference in reactivities. The overall reaction of complex **1** with O_2 to form complex **2** is the reverse of the reaction at the water-oxidizing complex of photosystem II (PS II). The four Mn/dioxygen, four-electron redox reaction feature of the reaction complex **1** + O_2 → complex **2** is relevant to the chemistry of the water-oxidizing complex. Also the dinuclear unit structure and the UV−visible absorption spectrum of **2** are features with relevance to the active site of manganese catalase.

Introduction

Intense interest[1] has been shown in manganese cluster complexes because of the role of such complexes at the active sites in various biological systems such as manganese catalase,[2] ribonucleotide reductase,[3] and the photosynthetic water-oxidizing enzyme photosystem II (PS II) in green plants and algae.[4] While manganese catalase and ribonucleotide reductase involve two Mn ions per molecule, PS II requires four manganese ions per molecule for activity. The manganese catalase in *Lactobacillus plantarum*[5] has been shown to contain μ-oxo bis(μ-carboxylato) bridging. Catalases disproportionate hydrogen peroxide while synthetic dinuclear Mn complexes are known with peroxo coordination[6] as well as di- and tetranuclear Mn complexes that show catalase-like activity.[7]

The early findings by Kok and co-workers[8] have shown that the Mn cluster in PS II undergoes four one-electron oxidation

* To whom correspondence should be addressed.
† Howard University.
‡ Centre National de La Recherche Scientifique.
⊗ Abstract published in *Advance ACS Abstracts,* May 15, 1995.

(1) (a) Christou, G. *Acc. Chem. Res.* **1989**, *22*, 328. (b) Wieghardt, K. *Angew. Chem.* **1989**, *101*, 1179; *Angew. Chem., Int. Ed. Engl.* **1989**, *28*, 1153. (c) Vincent, J. B.; Christou, G. *Adv. Inorg. Chem.* **1989**, *33*, 197. (d) Amesz, J. *Biochim. Biophys. Acta* **1983**, *726*, 1. (e) Pecoraro, V. L.; Baldwin, M. J. *Chem. Rev.* **1994**, *94*, 807. (f) DeRose, V. J.; Mukerji, I.; Latimer, M. J.; Yachandra, V. K.; Sauer, K.; Klein, M. P. *J. Am. Chem. Soc.* **1994**, *116*, 5239. (g) Dave, B. C.; Czemuszewicz, R. S. *New J. Chem.* **1994**, *18*, 149. (h) Proserpio, D. M.; Rappe, A. K.; Gorun, S. M. *Inorg. Chim. Acta* **1993**, *213*, 319.
(2) (a) Fronko, R. M.; Penner-Hahn, J. E.; Bender, C. J. *J. Am. Chem. Soc.* **1988**, *110*, 7554. (b) Allgood, G. S.; Perry, J. J. *J. Bacteriol.* **1986**, *168*, 563.
(3) Glenn, J. K.; Akileswaran, L.; Gold, M. H. *Arch. Biochem. Biophys.* **1986**, *251*, 688.
(4) (a) Brudvig, G. Q.; Beck, W. F. *Annu. Rev. Biophys. Biophys. Chem.* **1989**, *18*, 25. (b) Beck, W. F.; Brudvig, G. W. *J. Am. Chem. Soc.* **1988**, *110*, 1517. (c) Dismukes, G. C. *Photochem. Photobiol.* **1986**, *43*, 99. (d) Brudvig, G. W.; Crabtree, R. H. *Proc. Natl. Acad. Sci U.S.A.* **1986**, *83*, 4586. (e) Murata, N.; Miyao, M.; Omata, T.; Matsunami, H.; Kuwabara, T. *Biochim. Biophys. Acta* **1984**, *765*, 363.
(5) Fronko, R. M.; Penner-Hahn, J. E.; Bender, C. L. *J. Am. Chem. Soc.* **1988**, *110*, 7554.
(6) Bossek, U.; Weyhemuller, T.; Wieghardt, K.; Nuber, B.; Weiss, J. *J. Am. Chem. Soc.* **1990**, *112*, 6387.
(7) (a) Naruta, Y.; Maruyama, K. *J. Am. Chem. Soc.* **1991**, *113*, 5395. (b) Nishida, Y.; Nasu, M. *Inorg. Chim. Acta* **1991**, *190*, 1. (c) Larson, E. J.; Pecoraro, V. L. *J. Am. Chem. Soc.* **1991**, *113*, 3810. (d) Larson, E. J.; Pecoraro, V. L. *J. Am. Chem. Soc.* **1991**, *113*, 7809. (e) Larson, E. J.; Riggs, P. J.; Penner-Hahn, J. E.; Pecoraro, V. L. *J. Chem. Soc., Chem. Commun.* **1992**, 102. (f) Shindo, K.; Mori, Y.; Motoda, K.; Sakiyama, H.; Matsumoto, N.; Okawa, H. *Inorg. Chem.* **1992**, *31*, 4987. (g) Gelasco, A.; Pecoraro, V. L. *J. Am. Chem. Soc.* **1993**, *115*, 7928.

0020-1669/95/1334-3633$09.00/0

state (S state) changes, S_0 to S_4. The S_4 state is unstable and reverts to S_0 by oxidizing two molecules of water and releasing O_2. In the oxidation state S_1, where Mn(III) ions[9] have been proposed, the enzyme can bind and oxidize amines and hydroxylamine with the reduction of the cluster to a superreduced S_{-1} state and release of Mn(II) ions.[10] The S_2 state is EPR active,[11] showing a multiline spectrum similar to that characteristically exhibited by synthetic bis(μ-oxo) dinuclear mixed-valent $Mn^{III}Mn^{IV}$ complexes.[12]

One mechanism that has been proposed[4,13] for the water-oxidizing activity in PS II involves the conversion of two coordinated OH^- or H_2O species into a bridging peroxo (O_2^{2-}) intermediate, on the reaction pathway eventually leading to oxidation to O_2. This is supported by the observation that, in the dark, the S_2 state of PS II shows catalase-like activity toward added H_2O_2,[14] suggesting an arrangement of manganese ions in PS II that is similar to that found in catalase. The mechanism of peroxide disproportionation activity by catalase model complexes has been shown to involve inner-sphere dinuclear manganese center–H_2O_2 interactions.[7c-e] A peroxo-bridged synthetic dinuclear Mn complex has also been reported.[15]

The O–O bond formation stage in the oxidation of water is a critical step in which the two coordinated O^{2-} or OH^- groups that bridge manganese ions in the cluster have to be brought together to form the bond. One possibility is the presence of two dinuclear manganese moieties with intermetal ion bridging within a unit.

Dinuclear units in which the two manganese ions are bridged by two to three ions that include O^{2-} in a bis(oxo) bridge[16] or O^{2-} along with carboxylates,[17] alkoxides, etc. are widely observed and are among the best characterized. Structures have also been reported in which such dinuclear units are then either directly bridged or connected through organic groups in a so-called "dimer of dimers" [16,18] arrangement to give a tetranuclear manganese center. Structurally characterized tetranuclear manganese complexes have been found in various geometric arrangements such as adamantane,[19] cubane,[20] and butterfly.[21] The oxidation state of the manganese in these compounds can vary from +2 to +4, and many involve mixed-valent manganese ions.

We report here the synthesis, structure, and extensive studies, including IR, UV–visible, NMR, and EPR spectroscopy, electrochemistry, and kinetic studies, of the new tetranuclear manganese(III) complex $[Mn^{III}_4L_2(\mu\text{-}O)_2(\mu\text{-}OAc)_4](ClO_4)_4\cdot 3CH_3NO_2$, **2**, with the ligand L = α,α'-bis(bis(2-pyridylmethyl)-amino)-*m*-xylene.

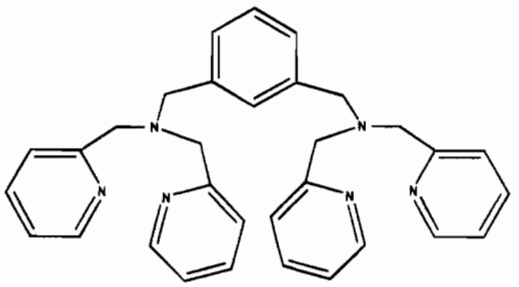

L

This complex is prepared by the controlled reaction of the precursor Mn(II) complex (complex **1**) of the ligand L with dioxygen at room temperature. Complex **2** contains two dinuclear manganese(III) coordination centers, linked by *m*-xylene spacing groups. Each dinuclear center is a (μ-oxo)bis-(μ-acetao)dimanganese(III) unit.

Experimental Section

Materials and Techniques. The reagents 2-(aminomethyl)pyridine, 2-(chloromethyl)pyridine, α,α'-dibromo-*m*-xylene, and $Mn(ClO_4)_2\cdot 6H_2O$ were used as received from Aldrich Chemical Co. Solvents used were all reagent grade solvents which had been further purified by refluxing over drying agents and distilled under nitrogen atmosphere. Ether was distilled from Na/benzophenone; acetonitrile was predried with P_4O_{10} and distilled from CaH_2; nitromethane was distilled from $CaCl_2$; methanol was distilled from $Mg(OCH_3)_2$. The synthesis of the Mn(II) complex was performed under nitrogen using vacuum/inert gas line and airless glassware techniques, and the product was stored under nitrogen. The high-purity-grade O_2 gas used in oxidation reactions was predried by passing the gas through a $CaCl_2$ drying tower. ^1H NMR spectra were taken on a GE 300 MHz spectrometer. Bis(2-pyridylmethyl)amine was synthesized according to the literature[22] method and purified by vacuum fractional distillation (bp 145–150 °C at 0.1 mmHg).

Synthesis of the Ligand α,α'-Bis(bis(2-pyridylmethyl)amino)-*m*-xylene (L). To a solution of α,α'-dibromo-*m*-xylene (1.33 g, 5.0 mmol) in THF (20 mL) was gradually added a solution of bis(2-pyridylmethyl)-amine (1.99 g, 10.0 mmol) and triethylamine (0.81 g, 10 mmol) in THF (20 mL), and the resulting mixture was stirred at room temperature over 24 h. The precipitate of $NEt_3\cdot HBr$ which formed was filtered off. The filtrate was rotary-evaporated and pumped under vacuum at 0.1 mmHg to remove all trace solvent and triethylamine. The golden brown clear oil obtained was shown to be pure by thin-layer chromatography (silica gel and alumina Baker Flex TLC plates in acetone solvent) and by NMR by a consistent peak area integration. ^1H NMR spectrum of L, chemical shift δ (multiplicity) (TMS = 0 ppm): 3.8 (s), 7.11 (m), 7.26 (m), 7.58 (m), 8.48 (m). UV–visible absorption spectrum in acetonitrile solution [λ_{max} (nm) (ϵ (M^{-1} cm^{-1}))]: 208 (4.58 × 10^2), 234 (5.13 × 10^2), 260 (5.25 × 10^2).

Synthesis of $Mn^{II}_2(L)(CH_3COO)_2(CH_3OH)(ClO_4)_2$ (1). A degassed solution of ligand L (2.50 g, 5.0 mmol) and CH_3COONa (0.82 g, 10.0 mmol) in methanol (40 mL) was added to a solution of $Mn(ClO_4)_2\cdot 6H_2O$ (3.61 g, 10.0 mmol) in degassed methanol (20 mL) under argon, and the mixture was stirred overnight. A colorless precipitate formed which was filtered off and washed with 20 mL of a methanol/

(8) Kok, B.; Rorbush, M. *Photochem. Photobiol.* **1970**, *11*, 457.
(9) (a) Sivaraja, M.; Philo, J. S.; Lary, J.; Dismukes, G. C. *J. Am. Chem. Soc.* **1989**, 3221. (b) Rutherford, A. W.; Boussac, A.; Zimmermann, J.-L. *New J. Chem.* **1991**, *15*, 491.
(10) Beck, W. F.; Sears, J.; Brudvig, G. W.; Kulaweic, R. J.; Crabtree, R. H. *Tetrahedron* **1989**, *45*, 4903.
(11) Ludwig, M. L.; Pattridge, K. A.; Stallings, W. C. *Metabolism and Enzyme Function*; Academic Press: New York, 1986; p 405.
(12) (a) Dismukes, G. C.; Siderer, Y. *Proc. Natl. Acad. Sci. U.S.A.* **1981**, *78*, 274. (b) Hannsom, O.; Andreasson, L. E. *Biochim. Biophys. Acta* **1982**, *679*, 261.
(13) Proserpio, D. M.; Hoffman, R.; Dismukes, G. C. *J. Am. Chem. Soc.* **1992**, *114*, 4347.
(14) (a) Frasch, W. D.; Mei, R. *Biochim. Biophys. Acta* **1987**, *891*, 8. (b) Mano, J.; Takahashi, M.; Aska, K. *Biochemistry* **1987**, *26*, 2495.
(15) Bossek, U.; Weyhemuller, T.; Wieghardt, K.; Nuber, B.; Weiss, J. *J. Am. Chem. Soc.* **1990**, *112*, 6387.
(16) Chan, M. K.; Armstrong, E. H. *J. Am. Chem. Soc.* **1991**, *113*, 5055.
(17) Pal, A.; Gohdes, J. W.; Wolf, C. C.; Wilisch, A.; Armstrong, W. H. *Inorg. Chem.* **1992**, *31*, 713.
(18) (a) Mikuriya, M.; Yamato, Y.; Tokii, T. *Chem. Lett.* **1991**, 1429. (b) Suzuki, M.; Hayshi, Y.; Munezawa, K.; Suenaga, M.; Senda, H.; Uehara, A. *Chem. Lett.* **1991**, 1929. (c) Mikuriya, M.; Yamato, Y.; Tokii, T. *Bull. Chem. Soc. Jpn.* **1992**, *65*, 2624.
(19) (a) Wieghardt, K.; Bossek, U.; Gebert, W. *Angew. Chem., Int. Ed. Engl.* **1983**, *22*, 328. (b) Wieghardt, K.; Bossek, U.; Nuber, B.; Weiss, J.; Bonvoisin, J.; Corbella, M.; Vitols, W. E.; Girerd, J. J. *J. Am. Chem. Soc.* **1988**, *110*, 7398.
(20) (a) Bashkin, J. S.; Chang, H.-R.; Streib, W. E.; Huffman, J. C.; Hendrickson, D. N.; Christou, G. *J. Am. Chem. Soc.* **1987**, *109*, 6502. (b) McKee, V.; Shepard, W. B. *J. Chem. Soc., Chem. Commun.* **1985**, 158. Li, Q.; Vincent, J. B.; Libby, E.; Chang, H.-R.; Huffman, J. C.; Boyd, P. D.; Christou, G.; Hendrickson, D. N. *Angew. Chem., Int. Ed. Engl.* **1988**, *27*, 1731.
(21) (a) Christmas, C.; Vincent, J. B.; Huffman, J. C.; Christou, G.; Chang, H.-R.; Hendrickson, D. N. *J. Chem. Soc., Chem. Commun.* **1987**, 1303. (b) Vincent, J. B.; Christmas, C.; Huffman, J. C.; Christou, G.; Chang, H.-R.; Hendrickson, D. N. *J. Chem. Soc., Chem. Commun.* **1987**, 236.
(22) Romary, J. K.; Bund, J. E.; Barger, J. D. *J. Chem. Eng. Data* **1967**, *1*, 224.

ether (1:1) mixture and then with 20 mL of ether. The colorless powder was dried under vacuum overnight and stored under argon (yield 2.65 g). Elemental analysis results support the formulation of the compound. Anal. Calcd for $C_{37}H_{42}O_{13}Cl_2N_6Mn_2$: C, 46.30; H, 4.38; N, 8.76; Mn, 11.45. Found: C, 46.45; H, 4.43; N, 9.00; Mn, 11.41. Infrared spectral data: peak centered at 3550 cm^{-1} due to ν_{OH} stretch (CH_3OH); 1602 cm^{-1} (pyridyl ring), 1450 and 1580 cm^{-1} (OCO bridging acetate). UV−visible absorption spectrum in acetonitrile [λ_{max} (nm) (ϵ (M^{-1} cm^{-1}))]: 234 (4.59 × 10^2), 260 (4.89 × 10^2), 290 (5.02 × 10^2).

Synthesis of $[Mn^{III}_4L_2(\mu\text{-}O)_2(\mu\text{-}OAc)_4](ClO_4)_4{\cdot}3CH_3NO_2$ (2). Complex **1** (1.00 g, 1.0 mmol) was dissolved in dry, degassed nitromethane (30 mL) under argon, and the solution was bubbled with dry O_2. The resulting solution was allowed to stir under an O_2 atmosphere at room temperature for 2−3 days. The dark brown color of the oxidation product **2** developed over time. The dark brown solution obtained was filtered under a dry O_2 atmosphere and a brown powder precipitated by addition of dry, degassed ether. Crystals suitable for X-ray crystallography were obtained by recrystallization from nitromethane/ether. Anal. Calcd for $Mn_4C_{75}H_{82}N_{15}O_{32}Cl_4$ C, 43.5; H, 4.15; N, 10.1; Mn, 10.6. Found: C, 43.67; H, 4.32; N, 9.73; Mn, 9.97. A sample of these crystals stored for more than a month at room temperature was also submitted for analysis and found to have a composition that best fits the formula without any solvent of crystallization (CH_3NO_2), showing that the solvent is lost over time. IR spectrum (Nujol): 1546 cm^{-1} (bridging acetate groups); 1602 cm^{-1} (pyridyl ring). Conductivity measurements made on acetonitrile solutions of complex **2** show values in the correct range for a 4:1 cation to anion charge ratio consistent with the formulation. Absorption spectrum in acetonitrile solution [λ_{max} (nm) (ϵ (M^{-1} cm^{-1}))]: 234 (1.24 × 10^3), 260 (1.27 × 10^3), 306 (1.29 × 10^3), 422 (4.45 × 10^2), 472 (3.60 × 10^2).

Magnetic Studies. Variable-temperature magnetic susceptibility data were obtained on powdered samples with a Quantum Design MPMS SQUID susceptometer. Diamagnetic corrections were applied by using Pascal's constants. Least-squares computer fittings of the magnetic susceptibility data were accomplished with an adapted version of the function-minimization program STEPT.[23]

Conductivity Measurements. A Fisher conductivity/pH meter apparatus with a YSI conductance cell (0.1 cm) was used in measuring the molar conductance of acetonitrile solutions of **1** and **2**. An Onsager plot was used to calculate the molar conductance of each complex based on measurements of the conductivities of solutions of each complex at four different concentrations (1.0, 0.8, 0.6, and 0.4 mmol).

Ultraviolet−Visible Spectrophotometry. All UV−visible absorption spectra of solutions of complexes were taken on a HP 8452 A diode array spectrophotometer equipped with a constant-temperature cell holder and interfaced with a 486/33 N Vectra HP computer. The sample solutions were held at constant temperature by circulation from a Fisher water bath/circulator, Model 9101. A special cell was constructed using a 1 cm path length quartz cell which had been modified by adding a 15 cm long cylindrical (1 cm diameter) glass tube (to provide extra volume for gaseous reactants). A ground-glass joint at the top of the tube enabled adaptation to a vacuum/inert gas line.

X-ray Crystallography. Crystals of complex **2** are readily obtained from dry nitromethane solution by layering with dry diethyl ether. However, we have learned from several attempts to determine the crystal structure that the compound loses crystallinity on standing at room temperature, as shown by the weak diffraction. This is due to the loss of the solvent of crystallization, as this is also reflected in the elemental analysis results for a fresh crystalline sample and a sample that has stood at room temperature for several weeks; the latter sample gives an elemental analysis that fits the formulation without any solvent (CH_3NO_2) of crystallization, while the elemental figures for the fresh sample are closer to those expected for a formulation with three molecules of solvent per tetranuclear unit.

A crystal of **2**, obtained by these methods, was glued to the end of a thin glass fiber with quick-setting epoxy cement and transferred to a Siemens P4S diffractometer. Crystal data for this complex are given in Table 1. Cell dimensions were obtained from the setting angles of 40 reflections in the range 12.5 < θ < 15°. Systematic absences indicated either the noncentrosymmetric space group $Pna2_1$ or the centrosymmetric space group *Pnma*. The latter space group was chosen on the basis of intensity statistics and the fact that the structure could be solved and refined successfully only in this space group. Since the crystals were not strong diffractors of X-rays, data were only collected for 2 < θ < 25°. A total of 8236 reflections were collected at low temperature (T = 173 K) using standard methods[24] giving a total of 7996 unique reflections. The structure was solved using automated Patterson methods and refined on F^2 by full-matrix least-squares methods.[25] The final R factors were 0.0880 (for those reflections greater than $2\sigma(I)$) and 0.1824 for all 7996 unique data.

Table 1. Summary of Crystal Data and Structure Refinement for Complex **2**

empirical formula	$C_{75}H_{85}Cl_6Mn_4N_{15}O_{40}$
formula weight	2269.04
temperature	173(2) K
wavelength	0.710 73 Å
crystal system	orthorhombic
space group	*Pnma*
unit cell dimensions	a = 24.755(5) Å, b = 28.854(4) Å, c = 12.495(2) Å, α = 90°, β = 90°, γ = 90°
volume	8925(3) $Å^3$
Z	4
density (calcd)	1.689 Mg/m^3
absorption coefficient	0.836 mm^{-1}
$F(000)$	4648
crystal size	0.48 × 0.39 × 0.26 mm
θ range for data collection	2.17−25.00°
index ranges	$0 \le h \le 29, 0 \le k \le 34, 0 \le l \le 14$
no. of reflections collected	7996
no. of independent reflections	7996 (R_{int} = 0.0000)
refinement method	full-matrix least-squares on F^2
data/restraints/parameters	7977/0/621
goodness-of-fit on F^2	1.063
final R indices [$I > 2\sigma(I)$]	R1 = 0.0880, wR2 = 0.1734
R indices (all data)	R1 = 0.1824, wR2 = 0.2351
extinction coefficient	0.00006(10)
largest diff peak and hole	+0.574 and −0.507 e $Å^{-3}$

Iodometric Titrimetric Determination of the Oxidation State of Mn in Complex 2. A sample of complex **2** (0.40 g, 0.2 mmol) was added to 25 mL of degassed and purged (N_2) water while a slow stream of nitrogen gas was maintained over the stoppered beaker. A yellow solution was obtained after 10 mL of concentrated sulfuric acid was added to dissolve the complex. A 1.006 g sample of KI was added, the solution was stirred, and then 5 mL of an indicator starch solution was added, turning the solution deep blue. The resulting solution was titrated against a standard thiosulfate solution (0.0400 M, also made in deoxygenated water) to the disappearance of the blue color, showing an end point at 9.8 mL.

The solution was warmed, and an additional 20 mL of concentrated sulfuric acid and 5 mL of starch solution were added, causing the blue color to reappear on stirring. On further titration with the thiosulfate solution, a second end point (disappearance of the blue color) occurred at 19.8 mL of the thiosulfate solution. The total volume of the standard thiosulfate solution at the second end point (at which time all Mn(III) had been reduced to Mn(II)) was then used to determine the mmol of I_3^- generated/mol of complex **2**.

Electrochemistry. Cyclic voltammetric measurements were obtained on the two complexes **1** and **2** in acetonitrile solution. A BAS CV-27 voltammograph equipped with a Faraday cage sample holding assembly and a recorder was used. In a typical experiment about 50 mg of the complex was dissolved in 5 mL of predried and nitrogen-purged acetonitrile. A continuous flow of nitrogen gas was maintained to form a blanket of inert gas over the solution throughout the experiment.

(23) Chandler, J. P. Program 66, Quantum Chemistry Program Exchange, Indiana University, 1973.

(24) Rowan-Gordon, N.; Nguyenpho, A. A.; Mondon-Konan, E.; Turner, A. H.; Butcher, R. J.; Okonkwo, A. S.; Hayden, H. H.; Storm, C. B. *Inorg. Chem.* **1991**, *32*, 4374.

(25) SHELXL93 (G. M. Sheldrick), a full-matrix least-squares refinement program based on F^2. The recommended weighting scheme for this program has the goodness-of-fit parameter tending toward 1.00 at the expense of the weighted R factor. Hence R_w = 0.1734 while the goodness-of-fit = 1.063 after final refinement.

Tetra-*n*-butylammonium perchlorate (0.01 mol/L) was used as the supporting electrolyte; a glassy carbon disk working electrode, a platinum wire auxiliary electrode, and a Ag/AgCl reference electrode (E = 0.19 V vs SHE) from BAS were used. Cyclic voltammograms were obtained in nonstirred solutions.

Determination of the Stoichiometry of the Reaction of the Mn(II) Complex 1 with O_2. a. Constant-Pressure Gas Manometry. A constant-pressure manometric glass apparatus[26] was used in which the U-tube, the buret, and the reaction flask (containing the dried solvent; 50 mL of CH_3NO_2 or CH_3CN) with a side arm connected to the buret (calibrated in mL) were filled with dried dioxygen gas at atmospheric pressure. The solvent was stirred for about 1−2 h to ensure that the solvent was saturated with O_2. The pressure of the gas was adjusted to atmospheric pressure by equalizing the mercury levels on the U-tube, and the mercury level in the buret was recorded.

The powdered manganese complex **1** (1.00 g, 1.0 mmol) contained in a storage tube fitted to the reaction flask (via a ground-glass joint) was emptied into the solvent and the stirring continued. The pressure of oxygen gas in the system was frequently readjusted to atmospheric pressure, as the pressure decreased as a result of oxygen gas uptake by the reaction. When constant pressure was reached (ca. 48 h), the mercury level was read and the volume of the oxygen gas taken up by the reaction calculated. The amount (mmol) of O_2 gas consumed by the reaction was calculated using the ideal gas law. After the experiment was repeated several times, it was found that an average of 0.48 ± 0.2 mmol of O_2 was consumed/mmol of the complex **1** dinuclear unit. The reaction product from these manometric experiments was isolated by precipitation by addition of dry ether and shown by its IR and UV−vis absorption spectrum to be the same as complex **2**.

b. Spectrophotometric Titration of O_2 vs the Mn(II) Complex. The titration was performed by mixing and reacting in a modified quartz cell with a total volume of about 40 mL. A regular quartz cuvette was modified by attaching a 10 cm long, 1 cm radius glass tubing to serve as added volume for gaseous reactants. To the top of this glass tube was attached a ground glass joint, with a Teflon needle valve, for airtight connection to an inert gas/vacuum system to facilitate the making of solutions under vacuum/inert atmosphere conditions and also to maintain an airtight seal of the reactants in the cell. A side arm was provided with a ground-glass joint fitted with a septum to enable reactants to be injected into the cell. After the cell had been taken through several vacuum/argon purge cycles to ensure an oxygen-free container, the cuvette was then evacuated. The solution of the Mn(II) complex was injected into the cell under vacuum, and several spectra of the initial solution were taken over several hours at the start of each experiment to ensure the stability of the starting Mn(II) complex and to make sure that the system was oxygen-free. A predetermined volume (at ambient temperature and pressure) of predried oxygen gas was injected into the cuvette via the septum at the top of the cuvette tube using a precision syringe. The mixture was then placed in a thermostated cell holder in the sample compartment of the spectrophotometer and vigorously stirred. The spectrum of the reaction mixture was taken in the 200−800 nm range at regular time intervals.

The reaction was followed for five different reaction stoichiometries. Five separate solutions were prepared, each with 0.25 g (0.25 mmol) of the Mn(II) complex **1** dissolved in 20.0 mL of deoxygenated dry CH_3CN under argon. To these solutions were added the following different volumes of O_2: (i) large excess amount of O_2 (30 mL at ambient temperature and pressure); (ii) 8.4 mL of O_2, 1.5:1 (mole ratio of O_2:**1**); (iii) 5.6 mL of O_2, 1:1 (mole ratio of O_2:**1**); (iv) 2.80 mL of O_2, 0.5:1 (mole ratio of O_2:**1**); (v) 1.4 mL of O_2, 0.25:1 (mole ratio of O_2:**1**).

The progress of the reactions was followed spectrophotometrically by measuring the absorbance at 422 nm (λ_{max} for the product complex **2**) at 2−4 h intervals until there was no increase in absorbance readings. The reaction was considered complete when the absorbance readings remained unchanged over at least 12 h (usually after ca. 4.5 days at 25 °C). The absorbance at the plateau (A_∞) agreed with the value expected for a 6.25 mM solution of the expected reaction product complex **2** calculated from the molar absorptivity for **2** already predetermined for a pure sample. A plot of the values of A_∞ of each mixture against the O_2:**1** mole ratio reaches its maximum at the 0.5:1 mixture, with the 1:1 and 1.5:1 mixtures and the mixture with large excess of O_2 all showing A_∞ equal to that of the 0.5:1 mixture while the maximum for the 0.25:1 mixture was half the value obtained for the others, thus showing that O_2 and complex **1** react in a 1:2 mole ratio in the formation of complex **2**.

Spectrophotometric Studies of the Reaction of Complex 2 with PPh_3 in Acetonitrile. A solution of **1** (0.016 g, 0.16 mmol) in 10 mL of dry acetonitrile was saturated with O_2 in a 25 mL flask, and the solution was stirred for 4 days to ensure the conversion to **2**. At the end of the reaction, the UV−visible absorption spectrum of the reaction mixture showed peaks at 422 (absorbance = 0.73) and 472 nm. To this mixture was added PPh_3 (0.026 g, 0.098 mmol), and the resulting mixture was transferred into a quartz cuvette and stirred under argon. UV−visible absorption spectra were taken at 10−12 h intervals to follow the progress of the reaction by the disappearance of the absorbance peaks of complex **2** at 422 and 472 nm over 4 days.

In a separate experiment, to a solution of **2** (0.30 g, 0.15 mmol) in 20 mL of acetonitrile was added PPh_3 (0.24 g, 0.92 mmol), and the mixture was stirred under argon at room temperature for 3 days. The brown solution decolorized to a faintly brown solution. After rotary evaporation of the solvent, the residue was extracted with diethyl ether (3 × 10 mL) to remove the excess PPh_3. The residue was then extracted with toluene (3 × 10 mL) to remove O=PPh_3. Removal of the toluene by evaporation under vacuum gave 0.351 g (73% yield) of a colorless solid shown to be O=PPh_3 by the fact that its IR spectrum in Nujol matched that of an authentic sample of O=PPh_3, including that characteristic peak for the P=O stretch at 1118 cm^{-1}.

Kinetic Studies. The kinetics of the reaction of the Mn(II) complex **1** with O_2 in acetonitrile solutions was studied by monitoring the increase in absorbance at 422 nm due to the formation of complex **2**, the oxidation product (the same procedure detailed in the section on the determination of the stoichiometry of complex **1** and O_2).

(a) Determination of the Dependence of the Rate of the Reaction on [1]. In a typical experiment, 0.06 g (0.06 mmol) of the Mn(II) complex **1** was dissolved in 5 mL of deoxygenated acetonitrile in an evacuated 1.0 cm quartz cuvette, which was then placed in a cell holder with the solution stirred and maintained at constant temperature. The stability of the spectrum of the initial solution of complex **1** was monitored while the cuvette was allowed 1−2 h to come to complete thermal equilibrium. The cuvette (40 mL) was then filled with O_2 at atmospheric pressure, providing a large excess of O_2, and the absorbance of the reaction mixture at 422 nm was recorded at regular time intervals over the 3−4 day reaction period. The concentration of complex **2** was calculated from these absorbance readings. The values of $\ln\{[\mathbf{2}]_\infty - [\mathbf{2}]_0/[\mathbf{2}]_\infty - [\mathbf{2}]_t\}$ versus time (hours) or $\ln\{[\mathbf{1}]_t/[\mathbf{1}]_0\}$ versus time (hours) are plotted to test for pseudo-first-order dependence on [**1**], where the calculated $[\mathbf{1}]_t$ was based on the stoichiometry that 2 mmol of **1** generate 1 mmol of complex **2**.

(b) Determination of the Dependence of the Rate of the Reaction on [O_2]. In these experiments large excesses of complex **1** [25:1 and 12.5:1 mole ratios of complex **1**:O_2) were used. A 0.25 g (0.25 mmol) sample of complex **1** was dissolved in 10.0 mL of deoxygenated acetonitrile to make a 25.0 mM solution of **1**. The cuvette (2.8 mL) was evacvuated and completely filled with the solution of **1**. In two experiments, 2.8 μmol (62.7 μL) and 5.6 μmol (125 μL) O_2 were injected directly into the solutions to give 1.0 and 2.0 mM solutions of O_2, respectively (since the solubility of O_2 in acetonitrile is 8.1 ± 0.6 mmol/L at 25 °C,[27] these are less than saturated solutions of O_2). The procedure detailed in part a was followed. The concentrations of O_2 versus time were calculated from the measured absorbances at 422 nm (due to complex **2**) and the known stoichiometry of the reaction. Plots were made of $\ln\{[\mathbf{1}]/[\mathbf{1}]_0\}$ versus time (hours) which gave a straight line.

Results and Discussion

Synthesis of the Ligand L. The synthesis of the binucleating ligand **L** was achieved by first synthesizing the secondary amine ligand bis(2-pyridylmethyl)amine (bpa). The reaction of of bpa

(26) Chen, D.; Martell, A. E. *Inorg. Chem.* **1987**, *26*, 1026.

(27) Achord, J. M.; Hussey, C. L. *Anal. Chem.* **1980**, *52*, 601−602.

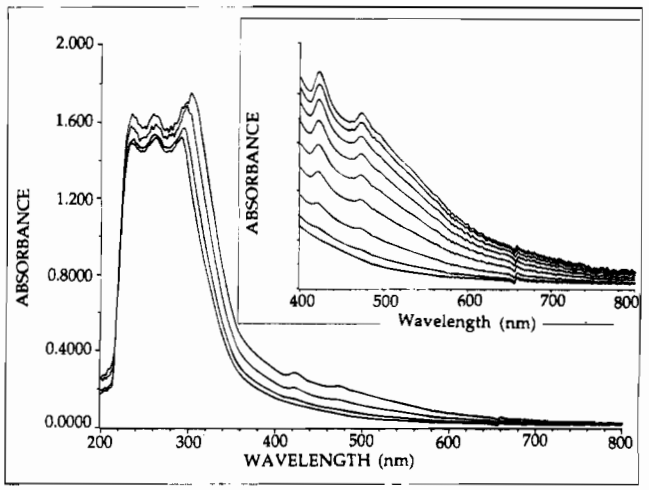

Figure 1. Ultraviolet−visible absorption spectra taken during the progress of the reaction of the Mn(II) complex **1** and O_2 in acetonitrile at 25 °C to form the Mn^{III}_4 complex **2**. The appearance and growth of the peaks at 422 and 472 nm are due to the formation of complex **2**. The starting Mn(II) complex **1** has no absorption peak in the visible region.

with α,α′-dibromo-*m*-xylene in a 2:1 mole ratio in THF in the presence of triethylamine base produced the ligand L in nearly quantitative yield in a highly pure form as shown by TLC and also by the ^1H NMR spectrum in $CDCl_3$. In our experience this method was more convenient than the alternative reaction of *m*-xylylenediamine and 2-picolyl chloride in the presence of sodium hydroxide in which side products (as judged by thin-layer chromatography) make the purification of the desired product difficult.

Synthesis of Complex 1. The reaction of $Mn(ClO_4)_2{\cdot}6H_2O$, the ligand L, and sodium acetate in methanol under argon gas precipitated the product complex as a colorless powder. The elemental analysis fits the empirical formula $[Mn_2L(CH_3COO)_2(CH_3OH)](ClO_4)_2$. The IR spectrum showed an absorption peak at 3450 cm^{-1} and can be assigned to a ν(OH stretch) consistent with the presence of methanol. Peaks observed at 1420, 1586, and 1602 cm^{-1} show the presence of acetate and pyridyl groups, respectively. A signal at $g = 2$ and a half-field peak near $g = 4$ in the EPR spectrum suggest the presence of magnetically coupled dinuclear centers. The room-temperature magnetic suceptibility of the powder sample is 5.7 μ_B per Mn, showing that the Mn ions are weakly antiferromagnetically coupled and most likely acetate bridged. Conductance measurements on a 1.0 mM solution of **1** in CH_3CN are consistent with a 2:1 electrolyte. The empirical formula $Mn_2L(CH_3COO)_2(CH_3OH)(ClO_4)_2$ is consistent with the elemental analysis, IR and EPr spectra, and conductivity data. Continuing attempts are being made to crystallize **1** in order to determine its structure, including the possibility that it might have a tetranuclear structure similar to its O_2 oxidation product complex **2**.

Reaction of Complex 1 and O_2. The reaction of O_2 gas with the manganese(II) complex **1** has been studied in the solvents acetonitrile and nitromethane. The reaction is slow and proceeds to completion over 3−4.5 days at room temperature. The colorless solution of **1** slowly develops an increasingly darker brown color with the progress of the oxidation reaction. Figure 1 shows UV−vis spectra taken while the reaction was in progress indicating the two peaks that appear and grow with time at 422 and 472 nm.

Unlike its precursor Mn(II) complex **1**, the crystalline product complex **2** shows no absorption in the 3300−3700 cm^{-1} region in its IR spectrum. The absorptions at 1602, 1586, and 1420 cm^{-1} due to the pyridyl and bridging acetate groups, respectively, are common to the IR spectra of the two complexes with the peak at 1586 cm^{-1} appearing stronger in the spectrum of complex **2** because of the additional absorption of nitromethane solvent of crystallization in this region. In addition, complex **2** shows a relatively stronger absorption peak at 720 cm^{-1} (assigned to the Mn−O−Mn asymmetric stretch) while only a relatively weak absorption peak is observed in that region of the IR spectrum of **1**.

The stoichiometry of the reaction of **1** with O_2 has been investigated using two methods: (a) constant-pressure manometric measurements of O_2 uptake; (b) spectrophotometric titration of **1** in acetonitrile with O_2. The manometric measurements show that 0.48 ± 0.02 mmol of O_2 is taken up/mmol of **1**. The product of this reaction was isolated and confirmed to be complex **2**. The spectrophotometric titration in which the ratio of O_2 to **1** was varied showed clearly that the stoichiometry of **1** + O_2 reaction was 2:1.

Iodometric Determination of the Oxidation State of Manganese in Complex 2. The iodometric determination of the oxidation state of Mn(III) is based on the known reaction involving the oxidation of I^- to I_3^- by Mn(III) with its own reduction to Mn(II) in strongly acidic solutions.[28] Two end points were obtained in the iodometric titration of **2** in acidified aqueous solution. In 2 M H_2SO_4 one end point corresponded to the generation of 1 mmol of I_3^-/mol of **2**, thus resulting in a two-electron reduction of the Mn^{III}_4 core, most likely resulting in two $Mn^{III}Mn^{II}$ centers. Further acidification of the solution to 5 M H_2SO_4 and further titration after the first end point showed a second end point corresponding to the generation of a further 1 mmol of I_3^-/mmol of **2**. This is most likely due to the further reduction of the previously generated $Mn^{III}Mn^{II}$ centers to the $Mn^{II}Mn^{II}_2$ complex.

$$[Mn^{III}Mn^{III}]_2 + 3I^- \rightarrow [Mn^{III}Mn^{II}]_2 + I_3^-$$

$$[Mn^{III}Mn^{II}]_2 + 3I^- \rightarrow [Mn^{II}Mn^{II}]_2 + I_3^-$$

These results indicate that complex **2** is a four-electron oxidant, which agrees well with the fomulation of the +3 oxidation state for all manganese ions in the tetramanganese unit. Further evidence for the +3 oxidation state for all Mn ions in complex **2** is furnished from other experiments, including (a) the establishment of the **1**/O_2 reaction stoichiometry as being 2:1, (b) the molar conductivity of **2** being consistent with a 4:1 electrolyte, (c) the charge balance requirements resulting from the X-ray structure determination, (d) the EPR-silent nature of **2** in a frozen-glass solution at liquid He temperature, and (e) the weak antiferromagnetic coupling between manganese centers calculated from the variable-temperature magnetic susceptibility studies which can be well modeled by assuming that the manganese centers are in the +3 oxidation state (see below).

Crystallographic Structure of Complex 2. Figure 2 shows the ORTEP drawing and perspective view of the cation $[Mn^{III}_4(\mu\text{-}O)_2(\mu\text{-}OAc)_4L_2]^{4+}$ of complex **2**. Complex **2** crystallizes in the orthorhombic group *Pnma* with four formula units per unit cell. There are three molecules of nitromethane of crystallization per formula unit $[Mn^{III}_4(\mu\text{-}O)_2(\mu\text{-}OAc)_4L_2](ClO_4)_4{\cdot}3CH_3NO_2$. The cation unit consists of two dinuclear coordination units connected by two *m*-xylene groups to form a tetranuclear center. A crystallographic mirror plane passes through the two *m*-xylene bridges. Each asymmetric unit consists of one-half formula unit of the cation, one whole and two half perchlorate ions (on mirror planes), and also one whole and one-half (also on a mirror plane) nitromethane molecules.[29]

Each dinuclear unit has two manganese ions, each coordinated by one amine and two pyridyl nitrogen donors of the ligand L

(28) Suzuki, M.; Murata, S.; Uehara, A.; Kida, S. *Chem. Lett.* **1987**, 281.

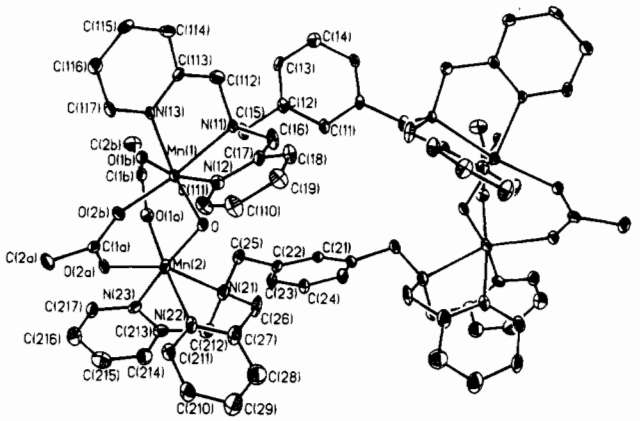

Figure 2. ORTEP plot of the cation $[Mn^{III}_4(\mu\text{-}O)_2(\mu\text{-}OAc)_4L_2]^{4+}$ of complex **2** showing the coordination structure and the atom-numbering scheme. The tetranuclear unit has a mirror of symmetry, and the halves of the cation are related by this symmetry. Hydrogen atoms are omitted for clarity.

and bridged by one oxo and two acetato groups. Each of these manganese ions is found in a distorted octahedral coordination geometry with a Mn(1)−Mn(2) distance of 3.261 Å. The two dinuclear units are separated from each other by a distance that is dictated by the rigid *m*-xylyl group connecting them. The Mn−Mn distance between two equivalent Mn ions in the two asymmetric half formula units of the cation related by the crystallographic mirror plane is 9.669 Å.

Table 1 gives the crystal data and details of the structure refinement. Atomic coordinates (Table 2) and bond distances and bond angles (Table 3) are given for the cation part of complex **2**. Deviations from 90 and 180°, respectively, in the *cis* and *trans* coordination angles make the coordination at each manganese a distorted octahedral geometry. These coordination angles at Mn(1) are also slightly different from those at Mn(2), with generally greater deviations from the expected octahedral angles in the Mn(2) coordination: O−Mn(2)−N(21), 101.2°; O−Mn(2)−O(2a), 99.9°; N(21)−Mn(2)−N(22), 73°. The corresponding angles at Mn(1) are 92.8°, 94.2°, and 79.4°. In addition, within a dinuclear unit, the coordination bond distances to Mn(2) are all longer than the bonds to Mn(1) by about 0.1 Å. The Mn−O(acetate) and Mn−N bond lengths of complex **2** are in the same range as those observed in other analogous dinuclear Mn(III) μ-oxo and bis(μ-acetato) dinuclear complexes[30] (see Table 5). The Mn−N(amine) distances for both Mn(1) and Mn(2) are significantly longer (2.265 and 2.307 Å) than the Mn−N(pyridyl) bonds (2.066−2.265 Å), which is attributable to the potential of pyridyl ligands to π-bond to metal ions, leading to shorter bond lengths.[31]

(29) Perchlorate groups 2 and 3 are disordered such that three of the four oxygen atoms on these groups lie on the mirror planes. Thus, while there are three perchlorate groups per dimeric asymmetric unit, the total multiplicity of the perchlorate groups is 2, consistent with the requirement by the charge balance considerations in the formula of complex **2**. Of the two solvent molecules (CH_3NO_2) in the asymmetric unit, one has the carbon (C(1N)) and nitrogen (N(1N)) on a mirror plane; hence only half of this molecule is in an asymmetric unit. Therefore, the total multiplicity is 1.5 solvent molecules per dinuclear asymmetric unit or 3 solvent molecules per tetranuclear unit.

(30) (a) Wieghardt, K.; Bossek, U.; Ventur, D.; Weiss, J. *J. Chem. Soc., Chem. Commun.* **1985**, 347. (b) Sheats, J. E.; Czemuczewicz, R. S.; Dismukes, G. C.; Rheingold, A. L.; Petrouleas, V.; Stubbe, J.; Armstrong, W. H.; Beer, R. H.; Lippard, S. J. *J. Am. Chem. Soc.* **1987**, *109*, 1435. (c) Menage, S.; Girerd, J.-J.; Gleizes, A. *J. Chem. Soc., Chem. Commun.* **1988**, 431. (d) Arulsamy, N.; Glerup, J.; Hazell, A.; Hodgson, D. J.; McKenzie, C. J.; Toftlund, H. *Inorg. Chem.* **1994**, *33*, 3023. (e) Oberhausen, K. J.; O'Brien, R. J.; Richardson, J. F.; Buchanan, R. M.; Costa, R.; Latour, J.-M.; Tsai, H.-L.; Hendrickson, D. N. *Inorg. Chem.* **1993**, *32*, 4561.

(31) Jones, C. M.; Johnson, C. R.; Asher, S. A.; Shepard, R. R. *J. Am. Chem. Soc.* **1985**, *107*, 3772.

Table 2. Atomic Coordinates ($\times 10^4$) and Equivalent Isotropic Displacement Parameters ($Å^2 \times 10^3$) for Complex **2**

	x	*y*	*z*	*U*(eq)[a]
Mn(1)	1163(1)	5824(1)	1453(1)	27(1)
Mn(2)	2476(1)	5754(1)	1575(1)	34(1)
Cl(1)	197(1)	3954(1)	2871(2)	61(1)
Cl(2)	1761(2)	7305(1)	3240(4)	42(1)
Cl(3)	817(2)	2678(2)	8369(5)	52(1)
O(11)	−371(3)	3992(2)	2664(6)	66(2)
O(12)	330(4)	4315(4)	3604(6)	121(4)
O(13)	296(3)	3514(3)	3303(7)	101(3)
O(14)	497(3)	4012(3)	1904(6)	80(2)
O(21)	1272(4)	7500	3597(10)	79(3)
O(22)	2215(4)	7500	3809(8)	59(3)
O(23)	1836(4)	7500	2123(9)	97(4)
O(24)	1722(5)	6808(4)	3409(10)	49(3)
O(31)	362(4)	2500	8830(11)	90(4)
O(32)	844(5)	2500	7263(11)	112(5)
O(33)	1300(4)	2500	8898(10)	75(3)
O(34)	764(5)	3159(4)	8464(13)	72(4)
N(11)	805(2)	6452(2)	627(5)	26(2)
N(12)	801(2)	6167(2)	2752(6)	33(2)
N(13)	388(2)	5591(2)	1158(5)	29(2)
N(21)	3030(3)	6394(2)	1424(6)	45(2)
N(22)	2711(3)	5947(2)	3214(6)	39(2)
N(23)	3253(3)	5460(2)	1231(6)	40(2)
O	1809(2)	6116(2)	1695(4)	32(1)
O(1a)	1304(2)	5236(2)	2375(5)	36(1)
O(2a)	2182(2)	5104(2)	2122(5)	38(2)
O(1b)	1389(2)	5564(2)	53(5)	36(1)
O(2b)	2290(2)	5627(2)	−24(5)	38(1)
C(11)	1188(4)	7500	−274(10)	33(3)
C(12)	1013(3)	7082(2)	740(6)	30(2)
C(13)	695(3)	7083(3)	−1657(7)	35(2)
C(14)	523(5)	7500	−2146(11)	48(4)
C(15)	1186(3)	6629(3)	−234(7)	36(2)
C(16)	713(4)	6794(3)	1477(7)	48(2)
C(17)	577(3)	6576(3)	2535(7)	33(2)
C(18)	272(4)	6801(3)	3292(7)	43(2)
C(19)	218(4)	6617(3)	4283(8)	47(2)
C(110)	463(4)	6201(3)	4510(8)	53(3)
C(111)	737(4)	5983(3)	3726(7)	45(2)
C(112)	284(3)	6303(3)	125(9)	48(3)
C(113)	52(3)	5883(3)	654(6)	31(2)
C(114)	−489(3)	5776(3)	522(7)	39(2)
C(115)	−678(3)	5360(3)	894(7)	41(2)
C(116)	−335(3)	5055(3)	1390(8)	43(2)
C(117)	194(3)	5188(3)	1517(7)	37(2)
C(21)	2966(4)	7500	434(9)	28(3)
C(22)	3200(3)	7076(3)	152(7)	33(2)
C(23)	3686(3)	7088(3)	−408(7)	40(2)
C(24)	3945(5)	7500	−676(10)	42(3)
C(25)	2904(4)	6619(3)	372(7)	39(2)
C(26)	2880(5)	6681(3)	2356(7)	60(3)
C(27)	2869(4)	6386(3)	3335(8)	57(3)
C(28)	3037(5)	6550(5)	4345(10)	79(4)
C(29)	3033(5)	6256(4)	5228(10)	82(4)
C(210)	2854(4)	5808(3)	5072(9)	55(3)
C(211)	2699(3)	5674(3)	4074(8)	43(2)
C(212)	3604(4)	6235(3)	1521(8)	53(3)
C(213)	3682(4)	5743(3)	1216(7)	46(2)
C(214)	4196(5)	5576(4)	1010(8)	61(3)
C(215)	4274(5)	5104(4)	846(9)	70(3)
C(216)	3825(4)	4817(4)	858(8)	58(3)
C(217)	3324(4)	5009(3)	1046(7)	45(2)
C(1a)	1731(3)	2994(3)	2461(7)	35(2)
C(2a)	1663(4)	4536(3)	3050(9)	51(3)
C(1b)	1835(3)	5584(3)	−464(7)	32(2)
C(2b)	1791(4)	5538(4)	−1644(7)	55(3)
O(1N)	1662(7)	2861(7)	1612(15)	230(7)
N(1N)	1427(14)	2500	1492(24)	180(10)
C(1N)	964(16)	2500	1267(39)	391(39)
O(21N)	2841(13)	1739(11)	2599(27)	401(17)
O(22N)	3289(8)	1225(8)	1112(18)	281(9)
N(2N)	3118(9)	1612(9)	1822(21)	210(9)
C(2N)	3394(14)	1936(12)	922(28)	359(20)

[a] *U*(eq) is defined as one-third of the trace of the orthogonalized $\mathbf{U}_{ij}$ tensor.

Table 3. Selected Bond Lengths (Å) and Bond Angles (deg) for Complex **2**

Mn(1)−O	1.834(5)	Mn(1)−O(1b)	1.984(6)
Mn(1)−N(13)	2.066(6)	Mn(1)−O(1a)	2.082(5)
Mn(1)−N(12)	2.101(7)	Mn(1)−N(11)	2.265(6)
Mn(2)−O	1.960(5)	Mn(2)−O(2b)	2.082(6)
Mn(2)−O(2a)	2.124(5)	Mn(2)−N(23)	2.145(7)
Mn(2)−N(22)	2.200(8)	Mn(2)−N(21)	2.307(7)
Mn(1)−O−Mn(2)	118.5(3)		
O−Mn(1)−O(1b)	94.2(2)	O−Mn(1)−N(13)	171.7(2)
O(1b)−Mn(1)−N(13)	89.0(2)	O−Mn(1)−O(1a)	97.9(2)
O(1b)−Mn(1)−O(1a)	97.5(2)	N(13)−Mn(1)−O(1a)	89.4(2)
O−Mn(1)−N(12)	91.6(2)	O(1b)−Mn(1)−N(12)	168.5(2)
N(13)−Mn(1)−N(12)	84.0(2)	O(1a)−Mn(1)−N(12)	91.6(2)
O−Mn(1)−N(11)	92.8(2)	O(1b)−Mn(1)−N(11)	90.7(2)
N(13)−Mn(1)−N(11)	79.4(2)	O(1a)−Mn(1)−N(11)	166.0(2)
N(12)−Mn(1)−N(11)	79.0(2)	O−Mn(2)−O(2b)	88.9(2)
O−Mn(2)−O(2a)	99.1(2)	O(2b)−Mn(2)−O(2a)	94.5(2)
O−Mn(2)−N(23)	168.9(2)	O(2b)−Mn(2)−N(23)	86.4(2)
O(2a)−Mn(2)−N(23)	91.3(2)	O−Mn(2)−N(22)	90.9(2)
O(2b)−Mn(2)−N(22)	174.6(2)	O(2a)−Mn(2)−N(22)	90.8(2)
N(23)−Mn(2)−N(22)	92.9(3)	O−Mn(2)−N(21)	94.5(2)
O(2b)−Mn(2)−N(21)	101.2(2)	O(2a)−Mn(2)−N(21)	159.4(3)
N(23)−Mn(2)−N(21)	76.5(3)	N(22)−Mn(2)−N(21)	73.5(3)

The Mn−N(pyridine) distance *trans* to the Mn−μ-O bond is slightly shorter (by 0.045 Å) than the *cis* Mn−N(pyridine) bond for both manganese centers. Such shortening of bonds *trans* to the Mn(III)−μ-oxo moiety has been observed in Mn(III) coordination in μ-oxo[30b] and μ-phenolato[32] dinuclear complexes. In μ-oxo Mn(III) complexes, this shortening has been attributed to the effect of the oxo ligand in raising the energy of the d_{z^2} orbital of Mn(III) (which is along the Mn−oxo direction) high enough to make it an empty orbital, thus shortening the bond to the *trans* ligand. This bond shortening effect is balanced by the expected Jahn−Teller elongation along the O−Mn−N_{trans} axis. This has the effect of keeping the Mn(III) coordination geometry rhombic rather than tetragonal, which usually results from Jahn−Teller elongation in Mn(III) d^4 systems. This rationale is also consistent with the very weak magnetic coupling observed in oxo-bridged Mn(III) complexes, including **2**. In this case, the weak coupling arises from the lack of the $d_{z^2}-d_{z^2}$ and $d_{z^2}-d_{xz}$ exchange pathways in the high-spin d^4 configuration where there is an empty d_{z^2} orbital. This is in clear contrast to the situation in high-spin Fe(III) d^5 ions in analogous dinuclear complexes where there is strong coupling due to the d_{z^2} orbital being occupied.[30b]

The Mn−O−Mn angle in **2** (118.4°) is within the range observed in analogous oxo- and diacetato-bridged dinuclear complexes (117−125°) and is similar to the angle in the analogous complex of the ligand TACN (117.8°; see Table 4). The Mn- - -Mn distance in **2** (3.261 Å) is longer than the distances observed in other oxo and diacetato triply bridged Mn(III) complexes (3.15−3.18 Å) and closer to the distances observed in oxo and acetato doubly bridged Mn(III) complexes (3.250−3.276 Å).[30a,33] In the latter complexes, these increased separations result from the larger Mn−O−Mn angles (*ca.* 130°), in contrast to the situation in **2**, where the increased separation results, at least partially, from the longer Mn−μ-O distances.

It is also noteworthy that, in complex **2**, two significantly different Mn−oxo distances are observed (1.834(8) and 1.960(8) Å). The former bond length (Mn(1)−O) is in the upper range of Mn(III)−oxo bond lengths found in analogous μ-oxo bis(μ-acetato) dinuclear Mn(III) complexes (1.78−1.82 Å).[34] The other Mn(III)−oxo bond length is significantly longer and outside this range by about 0.1 Å. Mn(III)−μ-O bond lengths of this magnitude are observed in alkoxo-bridged complexes (1.883−2.353Å),[35−37] phenoxo oxygen-bridged complexes (1.899−1.957 Å),[33,38,39] and tetranuclear mixed-valent complexes with μ_3-O bridging (1.828−1.930 Å).[33,40,41] The unusually long Mn(2)−μ-oxo distance of 1.963 Å is part of the generally different geometries assumed by the two manganese ions in the oxo-bridged dinuclear unit of this complex. This includes both differences in bond angles (N−Mn−N angles are more compressed (about 79°) for Mn(1) compared to those for Mn(2) (about 92°)). Instances of the occurrence of two distinctly different coordination geometries within the same compound in the crystalline structures of Mn(III) complexes have been reported in the literature and have been attributed to the lattice forces that significantly influence the Jahn−Teller distortions that are expected in these d^4 complexes.[42] However the possibility of Mn(2) being in the +2 oxidation state can be excluded on many grounds. In addition to chemical and spectroscopic evidence which excludes the +2 oxidation state for Mn(2), the Mn−O and Mn−N distances observed about Mn(2) also make the +2 oxidation state unlikely for this complex since Mn(II)−O and Mn(II)−N distances are commonly observed to be in the range 2.1−2.3 Å.[41b,43] EPR spectra of mixed-valent Mn(II,III) complexes are well-known and show a 16-line (multiple-line) spectrum[44] at $g = 2.0$, similar to the spectra of mixed-valent Mn(III,IV) complexes.[45]

Infrared Spectroscopy. Complexes **1** and **2** both show in common three absorption peaks in their IR spectra at 1602 cm^{-1}, assigned to the pyridyl ring stretch, and at 1450 and 1586 cm^{-1}, assigned to bridging acetate groups. A broad peak centered at 3450 cm^{-1} is also observed for **1** (consistent with the presence of methanol, also indicated by the elemental analysis), but no peak is observed in the spectrum of **2**, showing the absence of any OH in **2**. The peaks at 1450 and 1586 cm^{-1} both appear stronger in the spectrum of complex **2**, which is attributable to the additional absorption of the CH_3NO_2 solvent of crystallization in this complex. A relatively stronger peak is observed for **2** at 720 cm^{-1}, assigned to the Mn−O−Mn asymmetric stretch, whereas only weak peaks are found in the region between 700 and 800 cm^{-1} for **1**, consistent with the presence of a bridging oxo ligand in **2** but not in **1**. Asymmetric stretch absorptions by M−O−M moieties, including those of Mn and

(32) Dirile, H.; Chang, H.-R.; Nilges, M. J.; Zhang, X.; Potenza, J. A.; Schugar, H. J.; Isied, S. S.; Hendrickson, D. N. *J. Am. Chem. Soc.* **1989**, *111*, 5102.
(33) (a) Wu, F.-J.; Kurtz, D. M., Jr.; Hagen, K. S.; Nyman, P. D.; Debrunner, P. G.; Vankai, V. *Inorg. Chem.* **1990**, *29*, 5147. (b) Goodson, P. A.; Hodgson, D. J. *Inorg. Chem.* **1989**, *28*, 3606.
(34) Menage, S.; Girerd, J.-J.; Gleizes, A. *J. Chem. Soc., Chem. Commun.* **1988**, 431.
(35) Mikuriya, M.; Torihara, N.; Okawa, H.; Kida, S. *Bull. Chem. Soc. Jpn.* **1981**, *54*, 1063.
(36) Larson, E.; Lah, M. S.; Li, X.; Bonadies, J. A.; Pecoraro, V. L. *Inorg. Chem.* **1992**, *31*, 373.
(37) Bertoncello, K.; Fallon, G. D.; Murray, K. S.; Tiekink, R. T. *Inorg. Chem.* **1991**, *30*, 3562.
(38) Chan, C. K.; Armstrong, E. H. *J. Am. Chem. Soc.* **1990**, *112*, 4985.
(39) Buchanan, R. A.; Oberhausen, K. J.; Richardson, J. F. *Inorg. Chem.* **1988**, *27*, 971.
(40) (a) Kulawiec, R. J.; Crabtree, R. H.; Brudvig, G. W.; Schultze; Gaule, K. *Inorg. Chem.* **1988**, *27*, 1309−1311. (b) Hursthouse, M. B.; Thornton, P. J. *J. Chem. Soc., Chem. Commun.* **1980**, 684. (c) Baike, A. R. E.; Howes, A. J.; Hursthouse, M. B.; Quick, A. B.; Thornton, P. *J. Chem. Soc., Chem. Commun.* **1986**, 1587.
(41) (a) Gultneh, Y.; Farooq, A.; Liu, S.; Karlin, K. D.; Zubeita, J. *Inorg. Chem.* **1992**, *31*, 3607. (b) Mabad, B.; Cassoux, P.; Tuchagues, J.-P.; Hendrickson, D. N. *Inorg. Chem.* **1986**, *25*, 1420.
(42) (a) Avdeef, A.; Costamagna, J. A.; Fackler, J. P., Jr. *Inorg. Chem.* **1974**, *13*, 1854. (b) Gregson, A. K.; Doddrell, D. M.; Healy, P. C. *Inorg. Chem.* **1978**, *17*, 1216.
(43) Dirile, H.; Chang, H.-R.; Nilges, M. J.; Zhang, X.; Potenza, J. A.; Schugar, H. J.; Isied, S. S.; Hendrickson, D. N. *J. Am. Chem. Soc.* **1989**, *111*, 5102.
(44) (a) Mabad, B.; Tuchagues, J. P.; Hwang, Y. T.; Hendrickson, D. N. *J. Am. Chem. Soc.* **1985**, *107*, 2801. (b) Dismukes, G. C.; Sheats, J. E.; Smegal, J. A. *J. Am. Chem. Soc.* **1987**, *109*, 7202.
(45) Cooper, S. R.; Dismukes, G. C.; Klein, M. P.; Calvin, M. *J. Am. Chem. Soc.* **1978**, *100*, 7248.

Table 4. Bond Distances (Å) and Angles (deg) of Complex **2** and Analogous Oxo- and Diacetato-Bridged Complexes

complex[a]	Mn−μ-O	Mn−O_a[b]	Mn−N_t[c]	Mn−N_c[d]	Mn−O−Mn	Mn···Mn	ref
2	1.834	2.082	2.066	2.101	118.5	3.261	this work
	1.960	2.124	2.145	2.200			
3	1.790	2.001	2.051	2.232	125.1	3.175	*e*
			2.133	2.106			
4	1.781	1.937	2.058	2.049	122.9	3.132	*f*
	1.784	2.331	2.067	2.060			
5	1.805	2.051	2.252	2.222	117.8	3.084	*g*
		2.061					
6[h]	1.827	1.949	2.133	2.115[i]	125.1	3.230	*j*
	1.814	2.001	2.117				

[a] **3** = $[Mn^{III}_2(\mu\text{-O})(OAc)_2(HB(pz)_3)_2]\cdot CH_3CN$; **4** = $[Mn^{III}_2(MeCOO)_2(H_2O)_2(bipy)_2]^{2+}$; **5** = $[Mn^{III}_2(\mu\text{-O})(OAc)_2(TACN)]^{2+}$; **6** = $[LMn^{III}(\mu\text{-O})(\mu\text{-}O_2CCH_3)_2Mn^{IV}L]^{3+}$, L = *N,N′,N″*-trimethyl-1,4,7-triazacyclononane. [b] Mn−$O_{acetate}$. [c] *trans* to the Mn−oxo bond. [d] *cis* to the Mn−oxo bond. [e] Sheats, J. E.; Czernuczewicz, R. S.; Dismukes, G. C.; Rheingold, A. L.; Petrouleas, V.; Stubbe, J.; Armstrong, W. H.; Beer, R. H.; Lippard, S. J. *J. Am. Chem. Soc.* **1987**, *109*, 1435. [f] Menage, S.; Girerd, J.-J.; Gleizes, A. *J. Chem. Soc. Chem., Commun.* **1988**, 431. [g] Wieghardt, K.; Bossek, V.; Ventur, D.; Weiss, J. *J. Chem. Soc., Chem. Commun.* **1985**, 347. [h] The X-ray diffraction structural data for this Mn(III,IV) mixed-valent complex obtained by the oxidation of the Mn(III,III) complex **5** above it in this table show no differences in the bonding distances and angles from the Mn(III) and Mn(IV) ions. [i] Average of two distances. [j] Wieghardt, K.; Bossek, U.; Bonvoisin, P.; Beauvillain, P.; Girerd, J.-J.; Nuber, B.; Weiss, J.; Heinze, J. *Angew. Chem., Int. Ed. Engl.* **1986**, *25*, 1030.

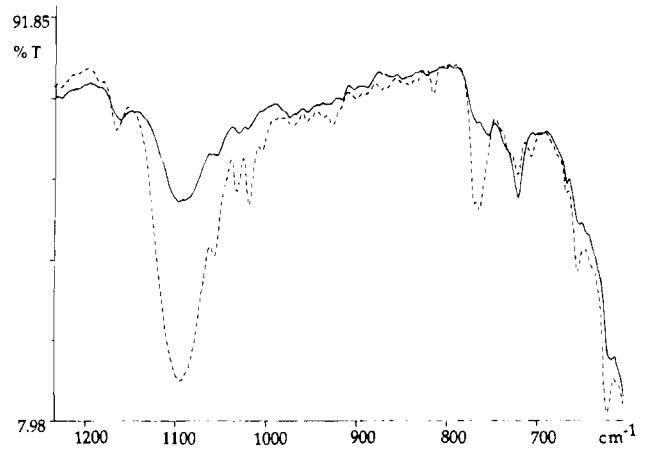

Figure 3. Infrared absorption spectra of samples of complex **2** (in Nujol) prepared by the oxidation of complex **1** in acetonitrile using isotopically pure $^{16}O_2$ (dashed line) and $^{18}O_2$ (solid line) showing the shift in the absorption due to the Mn−μ-O−Mn asymmetric stretch from 762 to 722 cm^{-1} as a result of isotopic shift, showing that the bridging oxo group originates from the O_2 used in the oxidation complex **1** to form complex **2**.

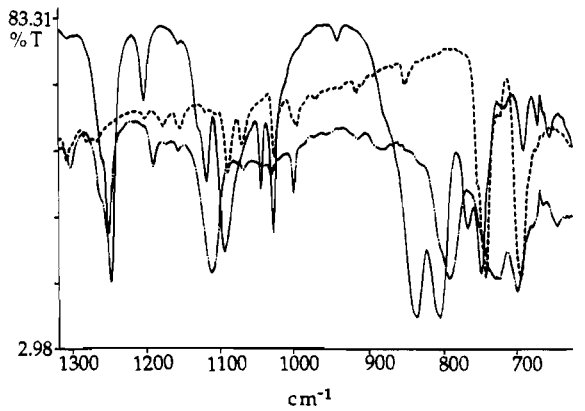

Figure 4. Overlay of the IR spectra (in Nujol) of PPh_3 (dashed line), O=PPh_3 (dotted line), and the product isolated after the reaction between complex **2** and PPh_3 (solid line). The appearance of the absorption at 1118 cm^{-1} (ν(P=O) stretch) indicates the formation of O=PPh_3 in this reaction as a result of the transfer of the bridging oxo group from complex **2** to PPh_3.

Fe, are usually observed in the region between 700 and 800 cm^{-1}, while the symmetric stretch is usually observed between 450 and 550 cm^{-1}.[30a]

The IR spectra of crystalline samples of complex **2** made by the separate reactions of **1** with $^{18}O_2$ and $^{16}O_2$ were studied to determine if the oxo bridge originated directly from the dioxygen reacted. Figure 3 shows an overlay of the spectra (in Nujol) of crystalline samples of complex **2** isolated from the reaction of **1** with isotopically pure $^{18}O_2$ and $^{16}O_2$ (**2**/$^{18}O_2$ and **2**/$^{16}O_2$). It is observed that the strong peak at 763.5 cm^{-1} in the spectrum of **2**/$^{16}O_2$ has diminished in strength in the spectrum of **2**/$^{18}O_2$ and a new strong peak appears at 721.7 cm^{-1} instead, which is assignable to the Mn−O−Mn asymmetric stretch. This shift of about 41 cm^{-1} in the Mn−O−Mn asymmetric stretch is to be expected[46] due to the isotope effect and has been found in the IR and resonance Raman spectra of oxo- and acetate-bridged dinuclear Mn(III) and Fe(III) complexes.[30b] These observations demonstrate that the bridging oxo group in complex **2** has its origin in the O_2 used in the oxidation reaction. To our knowedge, this is the first Mn(III) tetrameric complex with oxo bridging in which the bridging oxo group has been conclusively shown to originate directly from the reaction of a Mn(II) complex with O_2 and in which the oxo group is formed from the oxygen atoms that result from the reductive O=O bond breakage. From these facts, the implication can be drawn that O_2 is most likely directly coordinated to a multinuclear manganese center and that reduction and subsequent O−O bond breakage take place with the two oxygen atoms retained within the cluster to form the two oxo bridges at the two dinuclear sites in this tetramanganese cluster (see Scheme 1). This has significance in that the overall reaction is the reverse of the final stages of the water-oxidation reaction at the active site of PS II in which O−O bond formation and evolution of O_2 take place. A detailed study of the mechanism of this reaction could shed light on the mechanism of the oxidation of water by the water-oxidizing complex in PS II, including the coordination, electron transfer, and the critical O−O bond formation process.

Oxygen Atom Transfer from Complex 2 to PPh_3. Complex **2** was reacted with excess (1:4 mole ratio) triphenylphosphine (PPh_3) in acetonitrile overnight. Extraction of the residue with toluene and rotary evaporation gave a residual solid, the IR spectrum of which in Nujol showed a near peak at 1118 cm^{-1}, attributed to the P=O stretch of O=PPh_3, which is not observed in the IR spectra of control samples of **2** and PPh_3 (see Figure 4). However the reaction does not appear to be catalytic since addition of larger amounts of triphenylphosphine did not increase the amount of the oxide. We have also followed the reaction spectrophotometrically by measuring the intensity of the absorbance of **2** at 422 and 472 nm (λ_{max} of **2** assigned

(46) (a) Spool, A.; Williams, I. D.; Lippard, S. J. *Inorg. Chem.* **1985**, *24*, 2156. (b) Armstrong, W. H.; Spool, A.; Papaefthymiou, G. C.; Frankel, R. B.; Lippard, S. J. *J. Am. Chem. Soc.* **1984**, *106*, 3653.

Scheme 1. Proposed Mechanism of the Reaction of Complex **1** and O_2 in Acetonitrile To Produce Complex **2** Based on the Observed First-Order Dependence of the Reaction on the Concentration of O_2 and Complex **1**

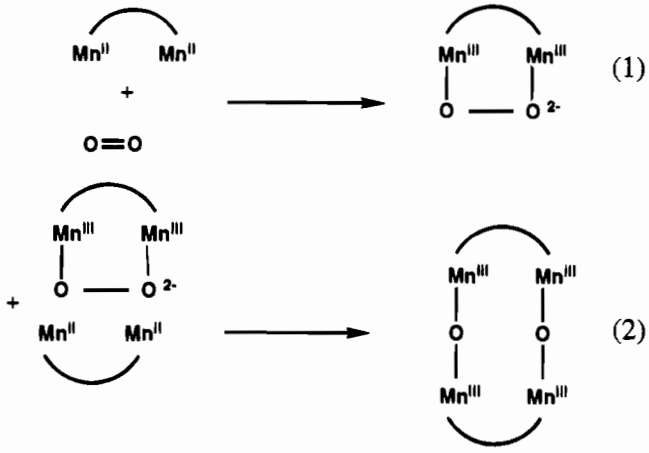

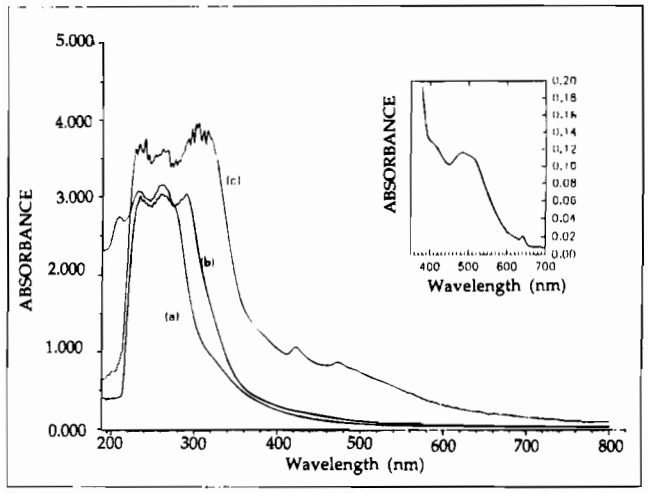

Figure 5. Ultraviolet−visible absorption spectra in acetonitrile solution of (a) the ligand L, (b) complex **1**, and (c) complex **2**. The inset is the spectrum in the visible region of the manganese catalase in *Lactobacillus plantarum* (Kono, Y.; Fridovich, I. *J. Biol. Chem.* **1983**, *258*, 6015, 13646).

to the oxo to Mn charge transfer absorption (see below)). The absorbance values at these wavelengths decrease as a function of time and virtually disappear over 3 days of the reaction at room temperature, indicating the reduction of **2** with the loss of the oxo group by transfer to PPh_3 to form $O{=}PPh_3$, which is also shown by the IR spectrum of the extracted product (ν(P=O) at 1118 cm^{-1}).

UV−Visible Absorption Spectroscopy. The UV−visible absorption spectra[47] of acetonitrile solutions of complexes **1** and **2** and the ligand L (Figure 5) all show strong bands in the UV region assigned to the $\pi-\pi^*$ transitions based on the pyridyl groups. From these spectra, it can be seen that complexation of the ligand L to form complex **1** causes the loss of the absorption peak of the ligand at 208 nm and the appearance of a new peak at 290 nm. This peak is then seen to shift gradually to longer wavelengths as the oxidation of **1** to **2** progresses until, after total conversion of **1** to **2**, the absorption maximum is observed at 307 nm. This effect is indicative of ligand π−metal

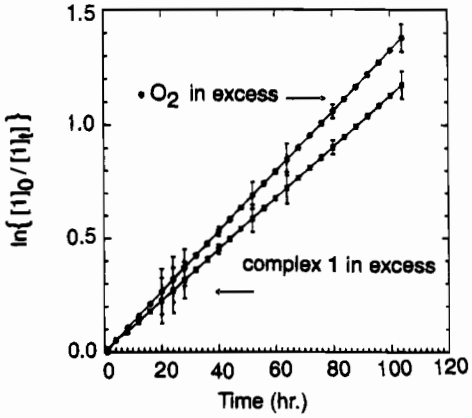

Figure 6. First-order plots for the dependence of the rate of the reaction of complex **1** and O_2 in acetonitrile on the concentration of complex **1** and on the concentration of dissolved O_2.

dπ interactions between the pyridyl aromatic system and the metal ion, which destabilize the ligand π molecular orbitals and decrease the $\pi-\pi^*$ energy gap, thus causing a bathochromic shift. This ligand π to metal dπ interaction has also been invoked to explain the short Mn−N_{py} bond lengths observed in the structure of complex **2** (see structure section). Complex **2** shows additional absorption bands at 422 and 472 nm, assignable to ligand to Mn(III) charge transfer transitions involving the oxo and acetato ligands. Resonance Raman enhancement of the Mn−μ-acetato mode by excitation at 457 and 488 nm for the analogous complex $[Mn^{III}_2(\mu\text{-}O)_2(\mu\text{-}OAc)_2(HB(pz)_3)_2]$ has demonstrated that absorptions in this region are LMCT transitions.[30b] These absorptions have also been observed in similar phenoxo oxygen-coordinated complexes of Mn(III).[48] In the spectrum of **2**, no absorption maximum was observed above 500 nm, unlike the case of the analogous tris(pyrazolyl)-hydroborate complex, which showed d−d absorption peaks in this region. However, it is possible that a weak absorption is obscured by the reletively strong charge transfer band.

Kinetic Studies. Spectra taken in acetonitrile kept saturated with O_2 during the progress of the reaction of **1** with O_2 over a period of 4 days at 25 °C are shown in Figure 1. The rate of the reaction of **1** with O_2 to form **2** was investigated spectroscopically by following the changes in absorptions at λ_{max} = 422 nm under conditions of excess O_2. A pseudo-first-order dependence of the rate of the reaction on the concentration of the dinuclear complex **1** was observed as evidenced by the straight line obtained on the plot of $\ln\{([\mathbf{2}]_\infty - [\mathbf{2}]_0)/([\mathbf{2}]_\infty - [\mathbf{2}]_t)\}$ vs time (hours) (Figure 6) or by taking the stoichiometrically calculated $[\mathbf{1}]_t$ (2 mmol of **1** generate 1 mmol of complex **2**) and plotting $\ln\{[\mathbf{1}]_0/[\mathbf{1}]_t\}$ versus time (hours). This strongly suggests that the rate-determining step is the formation of the complex between **1** and O_2. This is most likely a peroxo or a superoxo complex; i.e., step 1 in the reaction scheme shown is the slower and rate-determining step. Since the overall stoichiometry involves the reaction of 1 mol of O_2 with 2 mol of **1**, the second and faster reaction involves the complexation of a second dinuclear Mn(II) unit of **1**, with a further two-electron reduction leading to O−O bond breakage and the formation of the final product, **2**. The average value of the pseudo-first-order rate constant for the reaction of **1** with O_2 was found to be 2.8 ($\pm$0.4) × 10^{-4} M^{-1} s^{-1}.

Figure 7 represents the pseudo-first-order plots of data obtained from the studies of the reaction of complex **1** and O_2 at four different temperatures: 25, 40, 60, and 75 °C. The slopes

(47) The absorption spectra show the following [λ_{max} (nm) (ϵ (M^{-1} cm^{-1}))]. The ligand L: 208 (1.83 × 10^3), 234 (2.05 × 10^3), 260 (2.10 × 10^3). Complex **1**: 234 (1.98 × 10^3), 260 (1.99 × 10^3), 2.90 (2.01 × 10^3), 422 (1.57 × 10^2), 472 (8.70 × 10^1). Complex **2**: 234 (4.95 × 10^3), 260 (5.08 × 10^3), 306 (5.15 × 10^3), 422 (1.78 × 10^3), 472 (1.44 × 10^3).

(48) (a) Neves, A.; Erthal, S. M. D.; Vencato, I.; Ceccato, A. S.; Mascarenhas, Y. P.; Nascimento, O. R.; Horner, M.; Batista, A. A. *Inorg. Chem.*, **1992**, *31*, 4749. (b) Auerbach, U.; Eckert, U. Wieghardt, K.; Nuber, B.; Weiss, J. *Inorg. Chem.* **1990**, *29*, 938.

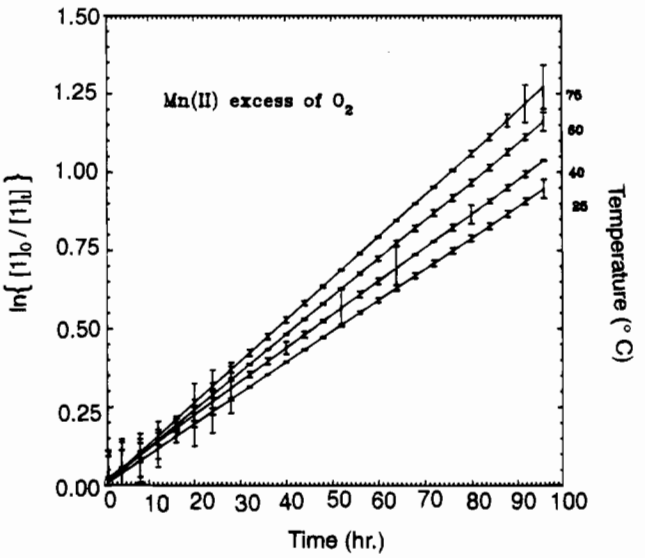

Figure 7. First-order plots of the rate of the reaction of complex **1** and O_2 in acetonitrile at different temperatures: 25, 40, 60, and 75 °C. The slopes of these straight lines were used to calculate the activation energy parameters (see text).

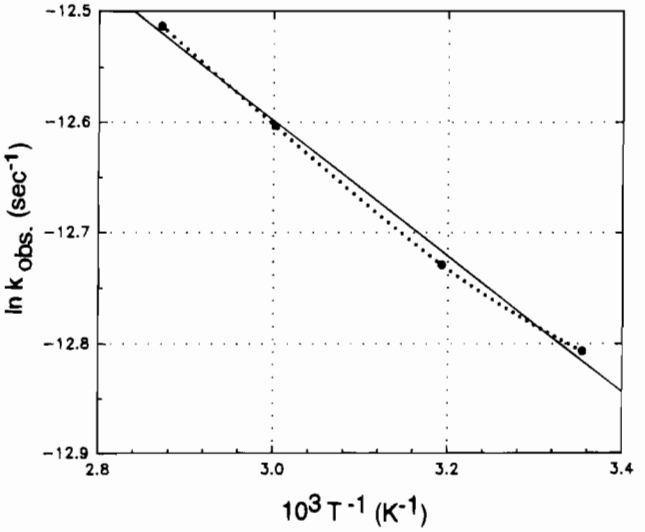

Figure 8. Arrhenius plot of the reaction of complex **1** with O_2 in acetonitrile. The slope of the straight line obtained in the plot gave the value of $-(E^{\ddagger}/R)$ from which the value $E^{\ddagger}$ (the activation energy) was calculated.

of the lines give the values of K_{obs} ($\times 10^6$ s^{-1}) as 2.742, 2.964, 3.360, and 3.678. The Arrhenius plot of $\ln(K_{obs})$ vs $1/T$ (Figure 8) gives a straight line from which a value for $E_a^{\ddagger}$ of 5.10 ± 0.05 kJ/mol was obtained. The Eyring equation was used to obtain the plot $\ln(K_{obs}/T)$ vs $1/T$ (Figure 9), which showed a straight line. The slope of this straight line gave the value of $-\Delta H^{\ddagger}/R$ of −294.5 (±0.1) K^{-1}, from which a value for $\Delta H^{\ddagger}$ of 2.45 ± 0.05 kJ/mol was obtained. From the intercept of this plot, a value was obtained for $\Delta S^{\ddagger}$ of −319 J K^{-1} mol^{-1}. From these values, a value was obtained for $\Delta G^{\ddagger}$ of 97.5 ± 0.2 kJ/mol at 298 K.

Electrochemistry. The cyclic voltammograms of complex **2** in unstirred acetonitrile solution are shown in Figure 10. Many electrochemical experiments have shown that **2** is highly unstable upon electrochemical reduction. Figure 10a shows the voltammogram with initial sweep in the cathodic direction. An irreversible reduction wave is observed at $E_p = -0.50$ V (versus Ag/AgCl) and is assigned to the reduction of the Mn(III)−O−Mn(III) complex to Mn^{II}_2, i.e. a two-electron reduction step. This conclusion is based on three observations: (i) Direct evidence for the reduction to the +2 oxidation state is obtained

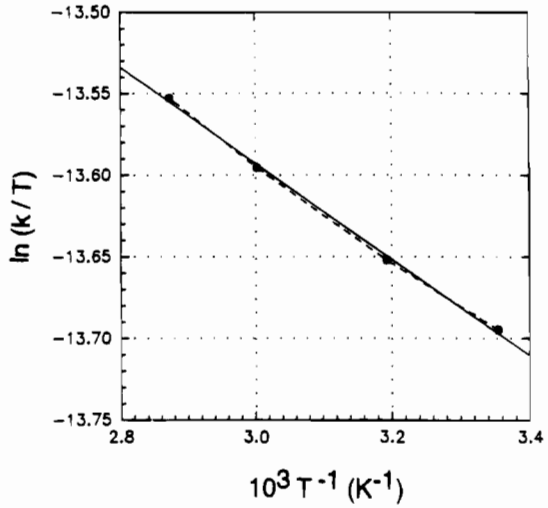

Figure 9. Eyring plot of the reaction of complex **1** with O_2 showing a straight line whose slope and intercept were used to calculate the values of the activation parameters $\Delta H^{\ddagger}$ and $\Delta S^{\ddagger}$, respectively (see text).

in the constant-potential reductive electrolysis at −0.50 V (versus Ag/AgCl) of a solution of **2** in acetonitrile in which the spectrum of **2** is observed to lose all absorption peaks in the visible region, as expected for the reduction of the Mn(III) ions in **2** to Mn(II). (ii) The reduction is totally irreversible, implying a drastic change in the complex and a loss of the bridging oxo on reduction (most likely due to the formation of OH^- in the presence of trace moisture). (iii) The following anodic sweep shows three waves at $E_p = 0.55$, 1.05, and 1.30 V (versus Ag/AgCl) which are assigned the processes $Mn^{II}_2 \rightarrow Mn^{II}Mn^{III}$, $Mn^{II}Mn^{III} \rightarrow Mn^{III}_2$, and $Mn^{III}_2 \rightarrow Mn^{III}Mn^{IV}$, respectively. The oxidation wave at $E_p = 0.55$ V has a corresponding reduction wave at $E_p = 0.45$ V, which makes this wave quasi-reversible. The 1.05 and 1.30 V oxidation waves are irreversible. The peak height (current) of the reduction wave for **2** (at $E_p = -0.50$ V) is roughly similar to the sum of the heights of the two oxidation processes, which supports the conclusion that the reduction of **2** is a two-electron reduction. The cyclic voltammetry of the Mn^{III}_2 complex of TACN also shows a simultaneous two-electron reduction from Mn^{III}_2 to Mn^{II}_2.[30a]

A similar, but somewhat different, phenomenon is observed in the voltammogram obtained by starting the scan in the anodic direction (see Figure 10b). Here, in the first cycle, an oxidation peak is observed at $E_p = 1.30$ V (versus Ag/AgCl), which is assigned to the oxidation of complex **2** to $[Mn^{III}Mn^{IV}]_2$. A relatively weak cathodic wave at $E_p = 1.10$ V is assigned to the reduction of this $Mn^{III}Mn^{IV}$ complex back to Mn^{III}_2. The reduction wave observed at $E_p = -0.15$ V is assigned to the reduction of Mn^{III}_2 to generate a Mn^{II}_2 species by another two-electron reduction. The following anodic cycle shows three waves at the same potentials as in Figure 10a and with the same assignments. After the first cycle, repetitive scans starting in either direction show in common the three oxidation waves and the cathodic wave at 0.45 V in Figure 10a,b. This behavior is indicative of the instability of **2** to reduction and its decomposition at the cathode surface to generate a new Mn(II) species that has its own redox potentials as observed on repetitive scans of the unstirred solution. Other corroborating evidence for the relative instability of the Mn−O−Mn entity especially toward reduction is provided by the fact that **2** is known to transfer the bridging oxo group to a reducing agent such as triphenylphosphine as discussed above. The unusually long Mn−μ-O distances in **2** also suggest a weak bond, and therefore easier removal of the oxo group may be likely under reductive conditions. This is also in agreement with the fact that other

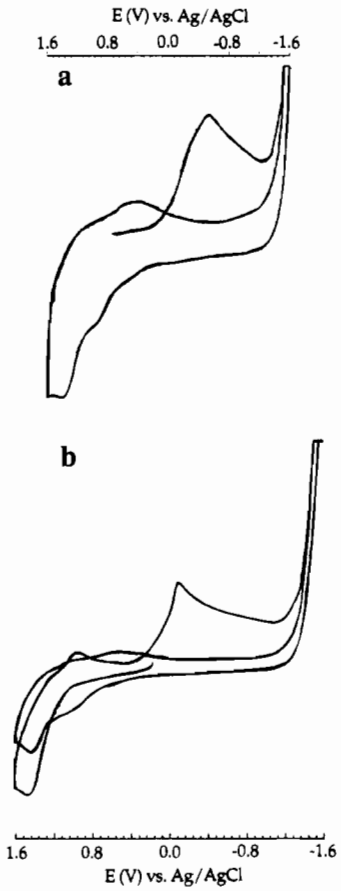

Figure 10. Cyclic voltammograms of complex **2** in acetonitrile solution: (a) initial scan in the cathodic direction; (b) initial scan in the anodic direction. The solution used is 0.10 M in complex **2** and 0.10 M in $[(n\text{-Bu})_4N]^+[ClO_4]^-$; a glassy carbon working electrode, a platinum wire auxiliary electrode, and a Ag/AgCl reference electrode were used.

analogous dinucleating ligands with bis(2-pyridylmethyl)amine (bpa) donor set arms are highly resistant to oxidation. Manganese(II) complexes analogous to **1** with ligands based on two bpa moieties linked by various aliphatic spacing groups $[(CH_2)_n$, where $n = 3-5$) are unreactive toward O_2 and, when reacted with aqueous H_2O_2, organic peroxides, or $KMnO_4$, produce yellow to brown solutions (presumably due to the oxidation of Mn) but revert back to the colorless Mn(II) complexes in solution, possibly by oxidizing the ligand itself or the solvent (methanol, acetonitrile, or dichloromethane).[49] It is remarkable that a change of the bridging group linking the bpa donor sets from a straight-chain alkyl group to a *m*-xylyl group makes the Mn(II) complex **1** reactive toward O_2, resulting in the formation of the Mn(III) complex **2**. This unique effect of the *m*-xylyl group bridge is likely to be due to its rigidity, which forces the two Mn(II) centers to a fixed distance in each dinuclear unit so that the molecules can then match their dinuclear centers for a concerted reaction with dioxygen and thereby kinetically facilitate the oxidation reaction; i.e., the entropic effect may be contributing the critical difference to drive the reaction of **1** with O_2 to form **2** whereas analogous complexes with flexible alkyl chain connections fail to react in a similar manner.

Quasi-reversible oxidation waves for the $Mn^{III}_2 \rightarrow Mn^{III}Mn^{IV}$ process and an irreversible cathodic wave for the reduction to Mn^{II}_2 have been observed for the analogous Mn(III)−O−Mn(III) complexes of the ligands $HB(pz)_3^-$ [30b] and TACN (1,4,7-triazacyclononane and *N,N′,N″*-trimethyl-1,4,7-triazacyclononane)[30a] (see Table 5). The structure of the electrochemical

(49) Gultneh, Y.; Karlin, K. D.; Butcher, R. J. Unpublished results.

Table 5. Cyclic Voltammeric Redox Potentials for **2** and Analogous Complexes

potential, V vs Ag/AgCl[a]	redox process	ref
1.$[Mn^{III}_2(\mu\text{-O})(\mu\text{-OAc})_2D_2]$		
D = *N,N′,N″*-Trimethyl-1,4,7-triazacyclononane		
$E_{1/2} = +1.11$ (q rev)	III,III → III,IV	*b*
$E_{pc} = +0.05$ (irrev)	III,III → II,II	
D = 1,4,7-Triazacyclononane		
$E_{1/2} = 0.81$	III,III → III,IV	*c*
$E_{pc} = -0.47$	III,III → II,II	
D = $HB(pz)_3^-$		
$E_{1/2} = 1.04$	III,III → III,IV	*d*
$E = -0.663$ (irrev)		
D = L (Bis(bis(2-pyridylmethyl)amino))-*m*-xylene (**2**)		
$E_{pa} = 1.30$	III,III → III,IV	this work
$E_{pc} = -0.50$ (irrev)	III,III → II,II	
2.$[Mn^{II}_2L(OAc)_2(CH_3OH)]^{2+}$		
L = α,α′-Bis(bis(2-pyridylmethyl)amino)-*m*-xylene (**1**)		
$E_{1/2} = 1.20$	II,II → II,III	this work

[a] Fc^+/Fc, $E = 0.537$ V versus Ag/AgCl (Gritzner, G. *Pure Appl. Chem.* **1982**, *42*, 1527. [b] Wieghardt, K.; Bossek, V.; Ventur, D.; Weiss, J. *J. Chem. Soc., Chem. Commun.* **1985**, 347. [c] Wieghardt, K.; Bossek, U.; Bonvoisin, P.; Beauvillain, P.; Girerd, J.-J.; Nuber, B.; Weiss, J.; Heinze, J. *Angew. Chem., Int. Ed. Engl.* **1986**, *25*, 1030. [d] Sheats, J. E.; Czernuczewicz, R. S.; Dismukes, G. C.; Rheingold, A. L.; Petrouleas, V.; Stubbe, J.; Armstrong, W. H.; Beer, R. H.; Lippard, S. J. *J. Am. Chem. Soc.* **1987**, *109*, 1435.

oxidation product, a $Mn^{III}Mn^{IV}$ complex, for the TACN complex has been reported.[50] Comparison of both the anodic potentials for these complexes to those of **2** show that the ligand L in **2** stabilizes the lower (III,III) oxidation state relative to the higher (III,IV) state of manganese compared to $HB(pz)_3^-$ and TACN. The anionic ligand $HB(pz)_3^-$ and the hard base amine nitrogens in TACN are both expected to stabilize the higher oxidation state compared to the neutral ligand L with its soft base pyridyl nitrogen donor atoms. The potential for the irreversible two-electron reduction of $Mn^{III}-O-Mn^{III} \rightarrow Mn^{II}_2$ in **2** (−0.50 V; see Figure 10a and Table 5) is comparable to the potential of an irreversible cathodic wave shown by the analogous complex of the ligand 1,4,7-triazacyclononane (−0.47 V vs Ag/AgCl), which the authors also assign to the two-electron reduction of the Mn(III,III) to the Mn(II,II) complex. However, the complex of *N,N′,N″*-trimethyl-1,4,7-triazacyclononane reported by Wieghardt et al. shows this irreversible reduction process at 0.05 V (about 0.4 V more positive than that for **2**). An irreversible reduction process is observed at $E = -0.663$ V (vs Ag/AgCl) for the complex of the anionic ligand $HB(pz)_3^-$, which as expected stabilizes the higher oxidation state better than the other ligands in this set.

Magnetic Properties of 2. The temperature dependence of the magnetic susceptibility and effective magnetic moment per manganese of **2** are shown in Figure 11. The effective magnetic moment per manganese ion decreases from 4.99 μ_B at 300 K to 2.98 μ_B at 3 K, indicating a weak antiferromagnetic coupling of the $S = 2$ spin systems of the two manganese(III) ions of each dinuclear unit and/or single-ion zero-field splitting (ZFS). Considering that the main distortion of the coordination octahedra around Mn(1) and Mn(2) can be described as a small compression along the $N(1)\cdots O_{oxo}$ axis (cf. X-ray molecular discussion), the individual *z* axes are oriented at an approximately 120° angle along these $N(1)\cdots O_{oxo}$ directions and the main superexchange pathway involves formally the d_{z^2} orbitals of Mn(1) and Mn(2). The structural evidence for axial compression supports a $^5A_{1g}$ ground state (*D* positive) with the

(50) Wieghardt, K.; Bossek, U.; Girerd, J. J.; Bonvoisin, J.; Beauvillian, P.; Weiss, J.; Nuber, B.; Heinze, J. *Angew. Chem.* **1986**, *98*, 1026.

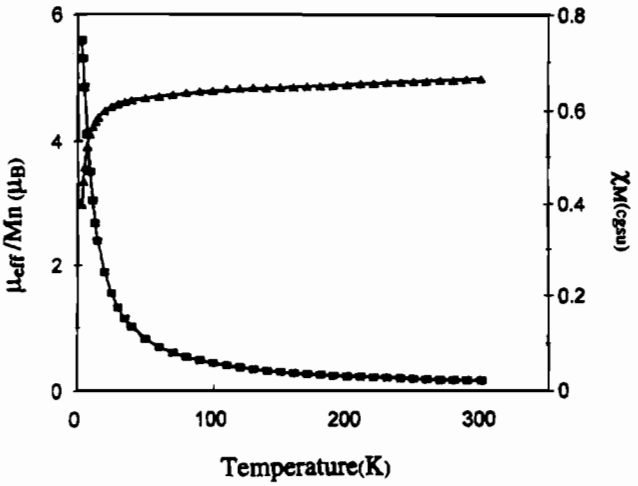

Figure 11. Plot of the variable-temperature magnetic susceptibility and magnetic moment of **2**. The solid lines result from a least-squares fit of the data to the theoretical magnetic susceptibility calculated as mentioned in the text.

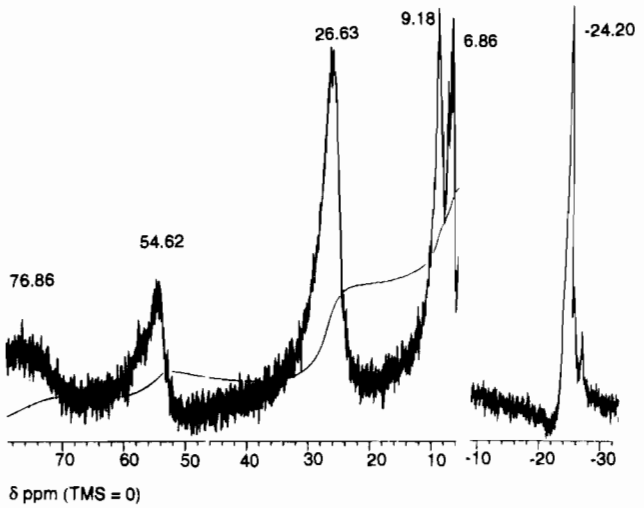

Figure 12. ^{1}H NMR spectrum of complex **2** in nitromethane-d_3 solution.

d_{z^2} orbital being highest and unoccupied. Hence, magnetic exchange interactions are probably ineffective for the $d_{z^2}-d_{z^2}$ and $d_{z^2}-d_{xz}$ pathways. Since the Mn(1)···Mn(2) distance (3.26 Å) is too large to allow direct overlap between orbitals, the only effective exchange involves probably superexchange between the $d_{x^2-y^2}$ orbitals through the acetate bridges. This rationale and the experimental results suggest that the magnetic exchange interactions in **2** are very weak, and the crystalline field anisotropy and the mangetic exchange interactions are expected to be of the same order of magnitude.

Consequently, the experimental data were fitted to the theoretical magnetic susceptibility calculated by exact diagonalization of the effective spin Hamiltonian taking into account single-ion ZFS.[51] The least-squares fitting of the experimental data to the theoretical magnetic susceptibility calculated from this model afforded a very good fit for the parameters $J = -0.4$ cm^{-1}, $D = 0.01$ cm^{-1}, $g_\perp = 1.895$, $g_\parallel = 2.008$, Par = 0, and TIP = 2×10^{-3}, where Par is the mole percent of a paramagnetic impurity assumed to be a Mn(III) monomer and TIP is the temperature-independent paramagnetism. The very small positive D value resulting from this analysis indicates that the single-ion ZFS terms are smaller than the isotropic exchange integral J by more than 1 order of magnitude.

The data were also fitted by employing the expression derived from the isotropic spin-exchange Hamiltonian $H = 2JS_1S_2$ ($S_1 = S_2 = 2$) and the van Vleck equation.[52] Least-squares refinement afforded an equally good fit (solid lines in Figure 11) with $J = -0.4$ cm^{-1}, $g_{av} = 1.941$, Par = 0, and TIP = 2×10^{-3}.

The very small exchange intergral J obtained for **2** is in the range, -4 to $+9$ cm^{-1}, of those previously obtained for the structurally characterized species containing the $Mn^{III}(\mu\text{-O})(\mu\text{-OAc})_2Mn^{III}$ core.[1b,53]

EPR Studies of 1. The structure of the Mn(II) precursor complex **1** has not yet been determined. The EPR spectrum of **1** shows a signal at $g = 2$ and a half-field peak near $g = 4$, suggesting the presence of magnetically coupled dinuclear centers. A six-line spectrum characteristic of monomeric species is attributed to the presence of a noncoupled manganese impurity that could arise from the dissociation of bridging acetate groups in solution. The room-temperature magnetic susceptibility of the powder sample is 7.2 μ_B per dinuclear formula unit, showing that the Mn(II) ions are antiferromagnetically coupled. In the infrared spectrum of complex **1**, absorption peaks at the frequencies characteristic of bridging acetate groups are observable. Whether this bridging is within a dinuclear unit comprising one ligand molecule or across two dinuclear units involving two ligand molecules and therefore a tetranuclear unit (vide infra) is not determined.

On the basis of the EPR spectrum of the S_2 state[54] and solvent relaxation effects,[55] the S_2 state of the water-oxidizing complex has been speculated to consist of a $Mn^{III}_3Mn^{IV}$ tetranuclear center. This leads to the conclusion that the S_1 state must have all the Mn ions in the +3 oxidation state.[56]

NMR Studies of 2. Complexes of Mn(III) are well-known to show ^{1}H NMR spectra due to their ligands with sharp peaks but large paramagnetic shifts.[57] The ^{1}H NMR spectrum of complex **2** in nitromethane-d_3 (Figure 12) shows broad absorption peaks in the chemical shift region δ -30 to $+70$ ppm (δ-(TMS) = 0.0 ppm), where analogous Mn(III) binuclear complexes are known to show absorptions,[31b] further confirming the +3 oxidation states of the Mn ions in the complex. The peak at 54.6 ppm is assigned to the methyl groups on the acetate bridges in analogy with similar peaks at 65.6 and 58 ppm for $[Mn^{III}_2(\mu\text{-O})(\mu\text{-OAc})_2(HB(pz)_3)_2]$[30b,52] and the mixed-valent complex $[Mn^{II}Mn^{III}(bpmp)(\mu\text{-O})(\mu\text{-OAc})_2](ClO_4)_2\cdot H_2O$ (bpmp = 2,6-bis((bis(2-pyridylmethyl)amino)methyl)-4-methylphenol),[43] which have been confirmed to be due to the bridging acetate methyl protons by isotopic studies. The peak at 26.6 ppm, the multiplets at 9.176 and 6.857 ppm, and the upfield-shifted peak at -24.2 ppm belong to the ligand protons. The ^{1}H NMR signals are broader than those of the analogous

(51) Garge, P.; Chikate, R.; Padhye, S.; Savariault, J. M.; De Loth, P.; Tuchagues, J.-P. *Inorg. Chem.* **1990**, *29*, 3315.
(52) O'Connor, C. J. *Prog. Inorg. Chem.* **1982**, *29*, 203.
(53) (a) Wieghardt, K. *Angew. Chem., Int. Ed. Eng.* **1989**, *28*, 1153. (b) Thorp, H. H.; Brudvig, G. W. *New. J. Chem.* **1991**, *15*, 479–490. (c) Vincent, J. B.; Tsai, H. L.; Blackman, A. G.; Wang, S.; Boyd, P. D.; Folting, W. K.; Huffman, J. C.; Lobkovsky, E. B.; Hendrickson, D. N.; Christou, G. *J. Am. Chem. Soc.* **1993**, *115*, 12353 and references therein.
(54) Guiles, R. D.,; Yachandra, E. K.; McDermott, A. E.; Britt, R. D.; Dexheimer, S. L.; Sauer, K.; Klein, M. P. *Prog. Photosynth. Res., Proc. Int. Congr. Photosynth., 7th* **1987**, *1*, 561.
(55) Srinivasan, A. N.; Sharp, R. R. *Biochim. Biophys. Acta* **1986**, *851*, 369.
(56) Christou, G.; Vincent, J. B. In *Metal Clusters in Proteins*; ACS Symposium Series 372; American Chemical Society: Washington, DC, 1988.
(57) Swift, T. J. In *NMR of Paramagnetic Molecules*; LaMar, G. N., Horrocks, W. DeW., Jr., Holm, R. H., Eds.; Academic Press: New York, 1973; pp 79–81.

complex of tris(pyrazolyl)hydroborate and about the same as those of other Mn(III) complexes.[58]

Conclusion

A tetranuclear Mn(III) complex has been synthesized and structurally characterized which is a dimer of dinuclear centers each with the μ-O,(μ-OAc)$_2$ motif. It has been demonstrated that a Mn(II) complex (with a probable dinuclear center) reacts under ordinary conditions with O_2 in a 4:1 Mn:O_2 molar stoichiometry to give rise to the tetranuclear Mn^{III}_4 complex. The oxidation states of all four manganese ions per molecule have been shown to be +3 by diverse methods, including redox titration, stoichiometry of the reaction of the precursor Mn(II) complex with O_2, molar conductance calculations, crystallographic data, and magnetic studies. The bridging oxo oxygens are shown to transfer to PPh_3, producing $O{=}PPh_3$, as shown by IR and spectrophotometric evidence. The kinetic data suggest the reaction is first order in the concentration of each of the two reactants **1** and O_2. The net reaction is a four-electron transfer from the four Mn ions to the O_2 molecule, resulting in O−O bond breakage and formation of two μ-oxo dinuclear Mn(III) centers. The retention of the oxygen atoms of the reacting dioxygen within the complex to form the bridging oxo ions has been demonstrated by isotopic labeling experiments. This combination of events in manganese chemistry is reminiscent of the last stages of the reactions of the water-oxidizing enzyme of the photosynthetic cofactor photosystem II, albeit in the reverse direction of reaction.

Although Mn−O_2 chemistry has been studied extensively, to our knowledge, this is the first example in synthetic manganese chemistry where this sequence of events has been demonstrated to take place at a tetranuclear Mn site and which has the four Mn−four electron redox reaction feature involving O_2 in common with the water-oxidizing complex in the biological system. The electrochemical activities of the tetranuclear Mn(III) complex **2** have been studied, demonstrating instability to reduction at the cathode. Attempts are being made to study further the chemical and electrochemical transformations of the Mn(III) complex and to isolate the products of such reactions in order to establish the structure of possible higher oxidation state derivatives of this system.

Acknowledgment. Y.G. wishes to thank Howard University for the support of this work through the Faculty Research Support Grant program. Y.G. also wishes to thank Professor Kenneth D. Karlin (Chemistry Department, The Johns Hopkins University) for the use of his laboratories for some of the earlier part of this work and for summer support through the National Institutes of Health. R.J.B. wishes to acknowledge the NIH-MBRS program for partial support of this work and the NSF for funding the purchase of the X-ray diffractometer. The help of Dr. Ralph Roberts (Chemistry Department, Howard University) in obtaining the ^{1}H NMR spectrum of the Mn(III) complex is acknowledged.

Supplementary Material Available: Tables of bond lengths and bond angles, anisotropic displacement parameters, hydrogen coordinates, and experimental and calculated magnetic susceptibilities and effective magnetic moments for complex **2** (6 pages). Ordering information is given on any current masthead page.

IC9501069

(58) Ramesh, K.; Bhuniya, D.; Mukherjee, R. *J. Chem. Soc., Dalton Trans.* **1991**, 2971−2974. Horrocks, W. DeW., Jr. In *NMR of Paramagnetic Molecules*; La Mar, G. N., Horrocks, W. DeW., Jr., and Holm, R. H., Eds., Academic Press: New York, 1973; pp 127−177.